TECTONICS, VOL. 7, NO. 6, PAGES 1339-1384, DECEMBER 1988

UNCERTAINTIES AND IMPLICATIONS OF THE LATE CRETACEOUS AND TERTIARY POSITION OF NORTH AMERICA RELATIVE TO THE FARALLON, KULA, AND PACIFIC PLATES

Joann Stock[1] and Peter Molnar

Department of Earth, Atmospheric, and Planetary Sciences, Massachusetts Institute of Technology, Cambridge

Abstract. We present updated global plate reconstructions and calculated uncertainties of the Pacific, Kula, and Farallon/Vancouver plates relative to North America for selected times since 68 Ma. Improved magnetic data from the Indian Ocean decrease the uncertainties in the global plate circuit approach; these uncertainties are now considerably smaller than those inherent in equivalent reconstructions based on the assumption of fixed hotspots. Major differences between these results and those of others are due to our use of more detailed Africa-North America reconstructions, separate Vancouver and Farallon plate reconstructions, and the assumption of a rigid Antarctica plate during Cenozoic time. The uncertainties in the relative positions of the Pacific and North America plates since the time of anomaly 7 (26 Ma) range up to ±100 km in position, or from 1 to 3 m.y. in time. If the Mendocino triple junction initiated at about 28.5 Ma, its position would have been at 31.3°N ± 130 km relative to fixed North America. Unacceptable overlap of oceanic crust of the Pacific plate with continental crust of western North America in the anomaly 10 (30 Ma) reconstruction is a minimum of 340±200 km along an azimuth of N60°E and may be accounted for by Basin and Range extension. Pacific-North America displacement in the past 20 Ma is found to be considerably less than that calculated by fixed hotspot reconstructions. Farallon (Vancouver)-North America convergence velocity decreased greatly between the times of anomalies 24 and 21 (56 to 50 Ma), prior to the 43 Ma age of the Hawaiian-Emperor bend and the often quoted 40 Ma "end" of the Laramide orogeny. A change in direction of Farallon-North America convergence occurred sometime between 50 and 42 Ma and also may not correlate with the time of the Hawaiian-Emperor bend. The lack of data from subducted parts of the Farallon and Kula plates permits many possibilities regarding the position of the Kula-Farallon ridge, the age of subducted crust, or the position of oceanic plateaus during the Laramide orogeny, leaving open the question of the relationship between plate tectonic scenarios and tectonic style during Laramide time. Displacements of points on the various oceanic plates along the west coast of an arbitrarily fixed North America during the interval between anomalies 30/31 and 18 (68 to 42 Ma) are found to be: Pacific plate,

[1]Now at Department of Earth and Planetary Sciences, Harvard University, Cambridge, Massachusetts.

Paper number 88TC03471.
0278-7407/88/88TC-0347$10.00

1700±200 km northward; Farallon plate, 3200±400 km northeastward; Vancouver plate, 3000±400 km northeastward; Kula plate, if attached to the Pacific plate after A24 time, 2500±400 km northward.

INTRODUCTION

The main postulate of plate tectonics, that plates of the lithosphere move with respect to one another as essentially rigid bodies, introduced the potential for quantitatively relating tectonic processes within continents to such motions. Immediately following the recognition of plate tectonics, considerable attention was paid to "geologic corollaries" that enabled geologists to read from the geologic record evidence for various plate tectonic settings, e.g., paired metamorphic belts as evidence of subduction or ophiolites as evidence of the creation of oceanic lithosphere. The quantitative relationships of known plate motions to reliably known geologic histories of large areas have been less successfully addressed; only the qualitative aspects, and not the quantitative basis, of plate tectonics have been exploited widely in geology.

Using plate tectonics as a constraint on the geologic evolution of most areas, or to deduce quantitative relationships, has not been easy. In many areas the presence of smaller plates, whose relative motions are poorly constrained, has limited the usefulness of well-constrained reconstructions of the major plates; the Mediterranean and Caribbean regions are examples. In other areas, such as between India and Eurasia, the geologic history is too poorly known to permit more than very simple and imprecise correlations between plate motions and geologic events. One of the geologically most promising areas to relate to plate motions is western North America, where important variations in tectonic style, rates of deformation, and magmatic patterns have occurred both along and across the western Cordillera. Atwater's [1970] study of the implications of plate tectonics for the tectonic evolution of western North America amply proves that plate motions are related in more than a superficial way to the tectonics of a neighboring continental area. Unfortunately it has not been possible to determine Pacific-North America relative plate motions adequately, except for the last 35 m.y. or so, and therefore there has been little progress since her study.

Several major stumbling blocks have limited the resolution of studies of plate motions in the northwest Pacific Ocean. One has been the obvious existence of an unknown plate boundary in the early Tertiary circuit of reconstructions, somewhere between the north Pacific and east Antarctica, but an inability to locate it and quantify motion across it. Another major difficulty, which has rendered virtually all studies of plate motions qualitative, at best, has been the lack of a reliable method for calculating uncertainties. The missing plate boundary seems to be in what is now the oceanic part of the Antarctica plate, and the relative motion across it can be estimated [Stock and Molnar, 1987]. Meaningful upper bounds on the uncertainties in the reconstructions, if not statistically rigorous confidence regions, can be assigned to all of the reconstructions using partial uncertainty rotations [Stock and Molnar, 1983; Molnar and Stock, 1985]. This paper incorporates these recent developments, with the following objectives: to present reconstructions of the Pacific, Kula, Farallon (Vancouver), and North America plates and bounds on their uncertainties and to examine some simple implications of the plate motions for the Tertiary evolution of western North America.

Over the past few years we have updated the rotation parameters describing the relative positions of the major lithospheric plates at different times in the Cenozoic era. We have tried to quantify their uncertainties in order to study the rates of motion among hotspots and the relationships of plate motions to the Cenozoic evolution of major convergent and strike-slip plate boundaries. Now that this data base is relatively complete, we present the reconstruction parameters for the major oceans and the application of these parameters to the study of the Tertiary history of western North America. Results bearing on the evolution of the Andean convergent zone [Pardo-Casas and Molnar, 1987], the Pacific-Australia strike-slip boundary in New Zealand [Stock and Molnar, 1987], and relative motions among hotspots [Molnar and Stock, 1987] have been published separately.

PREVIOUS WORK

The motion of the North American plate relative to oceanic plates west of it (Pacific, Kula, Farallon, and Vancouver) has long been recognized as a potentially important influence on the geologic evolution of western North America. Rates and directions of relative motion have been estimated by many previous workers, starting with Atwater [1970], who sought correlations between significant aspects of the plate motion history and events in the geologic record of western North America. These rates and directions have been obtained by two methods. Reconstructions made through the global plate circuit are based on matching sequences of magnetic anomalies on either side of a spreading center, in the sequence Pacific-Antarctica-Africa-North America or Pacific-Antarctica-India-Africa-North America [e.g., Atwater and Molnar, 1973; Jurdy, 1984]. These reconstructions have been useful for times younger than 42 Ma, but for earlier times discrepant results pointed to a missing plate boundary in the South Pacific or in Antarctica, so that this method could not be applied. An alternative method, based on the assumption that the hotspots are fixed to one another [Morgan, 1971; Wilson, 1963], yields reconstructions of the Pacific plate to North America using the sequence Pacific-hotspots-Africa-North America, with the central Atlantic magnetic anomalies constraining the reconstruction of Africa to North America [e.g., Coney, 1978; Engebretson et al., 1984b, 1985]. A variation of this technique is to reconstruct the Pacific plate directly to the North America plate by making assumptions about the motion of North America over the hotspots and then using the circuit Pacific-hotspots-North America [e.g., Carlson, 1982; Rea and Duncan, 1986; Verplanck and Duncan, 1987; Pollitz, 1988]. Results based on the fixed hotspot assumption are in rough agreement with the results from the global plate circuit, but a lack of knowledge of the uncertainties has made it both difficult to evaluate the significance of the differences between the results from the two methods and risky to compare these results with quantitative geologic observations.

Uncertainties in the marine magnetic reconstructions forming the global plate circuit must be known before the validity of a stationary hotspot reference frame can be demonstrated. Previous workers, lacking good estimates of the uncertainties in the marine magnetic reconstructions, came to vastly different conclusions regarding the rate of relative motion of the various hotspots [Burke et al., 1973; Duncan, 1981; Molnar and Atwater, 1973; Molnar and Francheteau, 1975; Morgan, 1981, 1983]. Even if hotspots were treated as relatively fixed, the uncertainties in the reconstructions of individual plates to hotspots could not be determined without knowledge of the uncertainties in the marine magnetic reconstructions used.

Many of our conclusions regarding rates and directions of motion of the Pacific, Kula, Farallon, and Vancouver plates with respect to North America do not differ in great detail from those obtained by previous workers, but important differences will be discussed. We do not give a lengthy discussion of the geology of western North America as it relates to plate motions because many detailed interpretations can be found elsewhere [e.g., Atwater, 1970, 1989; Atwater and Molnar, 1973; Coney, 1978; Dickinson, 1979; Dickinson and Snyder, 1979; Engebretson et al., 1984b, 1985]. We hope, however, that a knowledge of the uncertainties in these rates will allow geologists to evaluate the implications of the measurable changes in plate motions, as well as of the possible, but as yet unresolvable, variations and imprecisions in timings of changes, for the deformation observed on the North American continent.

DATA

Ship crossings of magnetic anomalies and fracture zones are the primary information used to obtain rotation parameters between pairs of plates and between different ages of crust on the same plate. These crossings were reevaluated from published ship tracks and digitized by us and coworkers for the Pacific [Molnar et al., 1975; Pardo-Casas and Molnar, 1987; Rosa and Molnar, 1988; Stock and Molnar, 1982, 1987] and Indian Oceans [Molnar et al., 1988; Stock and Molnar, 1982]. This list of points was augmented by a recent reanalysis of published and newly acquired ship tracks in the Atlantic Ocean [Klitgord and Schouten, 1986].

We attempted to maintain global consistency in the time in the geomagnetic reversal history corresponding to each anomaly we identify and consistent estimates of the uncertainty in the position of each digitized point. These uncertainties were assigned according to the quality of the magnetic or bathymetric signature, the navigation method, and agreement with adjacent tracks [Hellinger, 1981]. Uncertainties in position ranged from 4 km (for points from the best navigated and most closely spaced tracks in the central Atlantic and northeast Pacific oceans) to as much as 40 km for points from tracks recorded without satellite navigation in sparsely studied regions of the South Pacific and Indian oceans. Comparisons with synthetic magnetic anomalies suggest that the ages of the picks in the various oceans are consistent with the geomagnetic reversal time scale to within about ±0.15 Ma for ocean floor formed at slow spreading rates and are more consistent for fast spreading rates. This error is less than the spatial uncertainty in the data points and has not been explicitly included as an additional uncertainty in the reconstructions.

All possible identifications of Cenozoic magnetic anomalies 30/31, 25, 13, 6, and 5, according to Pitman et al.'s [1968] numbering system, were digitized for all of the spreading centers that we studied. In all oceans, at least one of anomalies 18, 20, and 21 was analyzed, and we interpolated to obtain the anomaly 18 and 21 reconstructions as necessary (see tables). For anomalies 7 and 10, we interpolated between adjacent reconstructions, assuming constant angular velocities. Positions of our picks on the magnetic reversal scale, and corresponding ages according to the commonly used time scales, are listed in Table 1. We use the Decade of North American Geology (DNAG) time scale of Berggren et al. [1985] and Kent and Gradstein [1985] for discussions and rate calculations in the text.

TABLE 1. Ages of Magnetic Anomalies Used

Anomaly	Position	Age,* Ma	Age,† Ma
5	old edge	10.59	10.48
6	center	19.90	19.96
7	center of larger reversal	25.82	26.11
10	center	30.03	30.83
13	center	35.58	37.07
18	center of broad normal epoch	42.01	42.29
20	center	45.51	44.90
21	center	49.55	48.08
23	center	54.29	51.70
25	center	58.94	55.96
28	center of reversed polarity interval between 28 and 29	65.31	63.80
30/31	center of reversed polarity interval between 30 and 31	68.47	66.93
33y	young edge	74.30 ‡	72.06
33o	old edge	80.17 ‡	78.53
34	young edge	84.00 ‡	82.93

* [Berggren et al., 1985]
† [Harland et al., 1982]
‡ [Kent and Gradstein, 1985]

DEPENDENCE OF THE RECONSTRUCTIONS ON THE TIME SCALE

We do not present reconstructions for equal time intervals because these require interpolation of reconstructions in the various oceans, based on the ages assigned to the magnetic polarity reversals. Hence they would require new interpolations and calculations for each time scale used and would introduce another level of uncertainty that would be difficult to quantify. Our reconstructions, except for anomalies 7 and 10, are made for specific positions in the sequence of magnetic reversals, so that they will be valid regardless of the times assigned to the polarity reversals by a particular time scale. All of the rates derived from the reconstructions depend on the time scale, and as the reversal chronology becomes better known, these inferred rates can be revised. Throughout the text we have tried to specify whether specific results depend on the choice of a time scale.

SINGLE RECONSTRUCTIONS AND THEIR UNCERTAINTIES

The past relative positions of adjacent diverging plates can be determined by matching crust of equivalent ages on both plates across the spreading center. For a given past time the relative position can be described mathematically as the rotation required to bring magnetic anomaly and fracture zone crossings of this age from the second plate into coincidence with those on the first plate. A variety of different techniques have been used to find the best rotation for a given set of points [e.g., Bullard et al., 1965; Chang, 1987; Engebretson et al., 1984a; Hellinger, 1981; McKenzie et al., 1970; McKenzie and Sclater, 1971; Nishimura et al., 1984; Pilger, 1978]. Some of these methods require estimation of the positions of intersections of magnetic anomalies and fracture zones, or estimation of isochron lines, rather than individual data points. Because such estimates are difficult to make in sparsely studied regions, and introduce additional complications to the calculation of the uncertainties, we use the method of Hellinger [1981], which requires only crossings of magnetic anomalies and fracture zones. This method minimizes the misfit of these points, weighted by their uncertainties, to great circles through segments of the plate boundary via an iterative search for the best pole position and angle. This method does not assume orthogonal spreading because the great circles fitting magnetic anomaly segments are not required to pass through a common point.

Because the uncertainties in latitude, longitude, and angle for each rotation are not independent, we describe the uncertainty in this best fit rotation in terms of "partial uncertainty rotations": three orthogonal small rotations that, when applied to the reconstructed boundary, result in the maximum acceptable misfit of the points from the two plates [Stock and Molnar, 1983]. These are calculated from the length and orientation of the plate boundary and the uncertainties in the positions of the magnetic anomalies and fracture zones. These small rotations can also be combined and expressed in terms of a "covariance" matrix for a perturbation of the best fit rotation [Chang, 1987; Jurdy and Stefanick, 1987]. In this paper we retain the uncertainties in rotation form so that the sources of uncertainty in the positions of reconstructed points can be identified easily.

If the magnetic anomalies from one plate of a spreading pair are missing, a "stage rotation" matching data points of two different ages can be computed from the anomalies on the other plate. We refer to this rotation as a "half-angle" stage rotation because it would represent half of the total motion between the two plates during the specified time interval, if spreading had been symmetric. The estimation of a "half-angle stage rotation" is mathematically equivalent to the estimation of a complete rotation (i.e., finding the best fit of two sets of points representing segments of a boundary of the same length and geometry). Thus for both single-sided and double-sided data, we use the same methods for determining best fits and uncertainties.

Reconstruction parameters for the South Pacific and Indian oceans, obtained using the methods described, are listed in Tables 2 to 13. Those for the central Indian ocean (Tables 7 to 9), North Pacific ocean (Tables 11-13), and central Atlantic ocean (Table 10) are reproduced and/or expanded from Molnar et al. [1988], Rosa and Molnar [1988], and Klitgord and Schouten [1986], respectively.

Of the plate boundaries we discuss there are two regions where half-angle stage rotations must be used: (1) in the northeast Pacific ocean, where magnetic anomalies from Pacific-Kula, Pacific-Farallon, and Pacific-Vancouver spreading remain only on the Pacific plate; and (2) in the southwest Pacific, where magnetic anomalies from Pacific-Antarctica spreading before the time of anomaly 18 have been surveyed on the Pacific plate south of New Zealand but not on the Antarctic plate [Stock and Molnar, 1987]. Assuming symmetric spreading without ridge jumps, complete rotations for these times are given by adding twice the half-angle stage rotation to the appropriate complete rotation for a later or earlier time, taking care to maintain the proper order of rotations. (See Table 14 for an example.) In these situations we use the half-angle stage rotation and its partial uncertainty poles twice.

An additional error due to asymmetric spreading or ridge jumps can neither be ruled out nor quantitatively evaluated and represents an additional problem in interpreting the results of reconstruc-

TABLE 2. Rotations and Uncertainties for Pacific to Antarctica

	"Best" Pole and Angle			End Points of Plate Boundaries and Azimuths of Transform Faults				
Anomaly	Lat*	Long*	Angle	Lat*	Long*	Lat*	Long*	Azimuth
5	72.00	-70.00	9.75	-35.83	-103.85	-63.01	-147.25	N70W
6	71.25	-73.19	15.41	-61.05	-140.26	-44.74	-101.13	N70W
13	74.83	-56.86	28.01	-55.59	-100.38	-61.63†	-133.62	N60W
18	75.08	-51.25	32.56	-53.97†	-97.41	-66.82†	-149.29	N62W

Best fit rotation parameters and uncertainties for the reconstructions used in this study. The uncertainties are described in terms of three "partial uncertainty rotations" corresponding to the three orthogonal rotation axes and the associated angle for unacceptable mismatch, treated here as a 95% confidence level [Stock and Molnar, 1983; Molnar and Stock, 1985]. The equivalent number of kilometers of mismatch at the plate boundary is also given. The magnetic anomaly ages correspond to the Decade of North American Geology [DNAG] time scale [Berggren et al., 1985; Kent and Gradstein, 1985].

* North and east are positive. Rotation angles are positive counterclockwise. Lat, latitude; Long, longitude.

† Endpoint rotated from the Pacific plate.

tions based on stage rotations. This is especially troublesome for times when the shape and/or orientation of the spreading ridge has changed during the time interval, as was the case for Pacific-Vancouver(Farallon) motion between anomalies 25 and 21 (Table 12). In this particular case we extrapolated from known rotations for earlier and later times, attempting to maintain a symmetric spreading configuration for isochrons reflected onto the Vancouver plate (Figure 2h). Despite the large uncertainties assigned to this rotation, it should be considered highly speculative.

COMBINED RECONSTRUCTIONS AND THEIR UNCERTAINTIES

Determination of Pacific-North America relative motion requires the combination of individual rotations to yield the relative motion of two nonadjacent plates. Combination of rotations in sequence is straightforward, but parameterizing the uncertainty in the resultant combined rotation is not [e.g., Chang, 1987]. We avoid this difficulty by parameterizing the uncertainty in final positions of rotated points, which provides more useful bounds on rates and directions of motion along a convergent or strike-slip boundary than the less easily visualized, mutually dependent uncertainties in latitude, longitude, and angle of the best rotation. In order to obtain the uncertainty in position of a single point we calculated the effect of each partial uncertainty rotation on this point and summed the contributions of all of the partial uncertainty rotations as two-dimensional Gaussian uncertainty distributions, treating the partial uncertainty rotation angles as corresponding to 95% confidence [Molnar and Stock, 1985]. Thus for each point we obtained an ellipse on a map, which we treat as a 95% confidence limit for the final position of the point.

Because the sizes of these uncertainty regions depend on the small rotation angles that we have chosen to yield allowable misfits for each of the partial uncertainty rotations, they are not statistically rigorous 95% confidence regions. We believe that the partial uncertainty angles are reasonable and that they are consistent with the quality of the locations of the magnetic anomalies

TABLE 2. (Continued)

Skewed Fit				Mismatched Fracture Zones				Mismatched Magnetic Anomalies			
Lat*	Long*	Angle, deg	Angle, km	Lat*	Long*	Angle, deg	Angle, km	Lat*	Long*	Angle, deg	Angle, km
-51.31	-119.14	0.55	20	12.34	166.72	0.18	20	35.97	-94.14	0.18	20
-54.46	-116.84	0.37	20	11.47	169.65	0.18	20	33.11	-92.74	0.18	20
-59.68	-115.52	1.14	20	14.62	-179.03	0.18	20	25.93	-81.75	0.18	20
-62.83	-117.84	0.38	20	12.38	177.47	0.18	20	23.78	-86.98	0.18	20

and fracture zones. Some readers may disagree with the values of the uncertainties we assigned to the data points, and future data collection will reduce these uncertainties, but confidence intervals based on other partial uncertainty rotation angles are easy to recalculate by this method.

SEQUENCE OF RECONSTRUCTIONS USED

Parameters describing motion of the Pacific plate with respect to North America were obtained using the Pacific-Antarctica-India-Africa-North America plate circuit for the time of anomaly 25 and the Pacific-Antarctica-Africa-North America plate circuit for other times (Table 14). Kula-North America, Farallon-North America, and Vancouver-North America rotation parameters were calculated using "stage pole" rotations on the Pacific plate [Rosa and Molnar, 1988] combined with the Pacific-North America rotations. For all times except 5.5 Ma the rotation parameters were either determined directly or interpolated from adjacent times. The 5.5 Ma (anomaly 3) Pacific-North America reconstruction is based on an extrapolation of Minster and Jordan's [1978] angular velocities, and associated uncertainties, for Pacific-Antarctica, Antarctica-Africa, and Africa-North America, from the RM-2 geohedron. Because these are finite rotations, this reconstruction for 5.5 Ma gives a slightly different result than would be obtained by direct extrapolation of the instantaneous Pacific-North America angular velocity vector. The uncertainty in this reconstruction includes the 5.5 Ma rotations extrapolated from the instantaneous Pacific-North America velocities of Minster and Jordan [1978] and of Chase [1978] but not that of DeMets et al. [1987].

We use the 5.5 Ma reconstruction to close the San Andreas fault system and the Gulf of California in Figure 2. This reconstruction restores 325 km of plate separation at the latitude of the Mendocino triple junction and 308 km at the mouth of the Gulf, but it is meant to be illustrative rather than rigorous. Because the 5.5 Ma reconstruction is based on extrapolation of younger data, rather than direct calculation, it is not used in our discussion or rate calculations.

DIFFERENCES BETWEEN GLOBAL RECONSTRUCTIONS AND FIXED HOTSPOT RECONSTRUCTIONS

In global reconstructions the Farallon plate is reconstructed to the North America plate by matching marine magnetic anomalies through the plate circuit Farallon-Pacific-Antarctica-(India)-Africa-North America. In fixed hotspot reconstructions the Pacific plate and either the North America or Africa plate are reconstructed to the hotspots beneath them (assumed fixed with respect to one another), but marine magnetic anomalies are used to reconstruct the Farallon plate to the Pacific plate and, in some cases, the North America plate to the Africa plate. In addition to the fundamental difference between these reconstruction paths the results of these methods may differ because of differences in rotation parameters for a given boundary, additional plates included in the plate

TABLE 3. Rotations and Uncertainties for Pacific to Bellingshausen

	"Best" Pole and Angle			End Points of Plate Boundaries and Azimuths of Transform Faults				
Anomaly	Lat*	Long*	Angle	Lat*	Long*	Lat*	Long*	Azimuth
25	71.61	-57.47	40.11	-60.02	-112.67	-65.38	-128.7	N52W
30/31	71.65	-49.00	53.75	-62.23	-106.08	-67.42	-125.88	N54W

See Table 2 footnotes.
* North and east are positive. Rotation angles are positive counterclockwise. Lat, latitude; Long, longitude.

TABLE 4. Rotations and Uncertainties for Antarctica to Australia

	"Best" Pole and Angle			End Points of Plate Boundaries and Azimuths of Transform Faults				
Anomaly	Lat*	Long*	Angle	Lat*	Long*	Lat*	Long*	Azimuth
5	8.70	35.56	6.65	-39.16	90.99	-59.28	155.63	0E
6	8.95	32.07	11.90	-37.90	95.13	-56.69	157.22	N2W
13	11.68	31.81	20.46	-25.70	82.37	-51.50	157.55	0E
18	8.68	34.52	22.80	-38.35	130.60	-50.25	156.15	0E
25	4.45	35.99	25.55	†	†	†	†	
30/31	3.76	36.23	26.08	†	†	†	†	

See Table 2 footnotes.
* North and east are positive. Rotation angles are positive counterclockwise. Lat, latitude; Long, longitude.
†These best fit poles were calculated by interpolation between the anomaly 18 pole [Stock and Molnar, 1982] and the magnetic quiet zone fit [König, 1980], using distances given by Cande and Mutter [1982]. Partial uncertainty rotation axes were rotated from anomaly 18, with angle value doubled to reflect additional uncertainty in these interpolated poles.

circuit, the relative motion of hotspots, and differences in the calibration of the ages of hotspot traces and magnetic field reversals.

The uncertainties in global plate reconstructions of Pacific-North America motion, for the times considered here, are smaller than the uncertainties in the equivalent fixed hotspot reconstructions derived from the parameters of Morgan [1981, 1983] or Duncan [1981]. This difference in size of uncertainties must be due to the Pacific-Africa part of the plate circuit, because the Africa-North America part of each circuit is the same. The error due to the assumption that the Pacific and African hotspots are fixed relative to one another [e.g., Duncan, 1981; Morgan, 1981, 1983] has generally been assumed to be 1-5 mm/yr. However, tests of hotspot fixity, based on recent reconstructions and realistic upper bounds

TABLE 3. (Continued)

Skewed Fit				Mismatched Fracture Zones				Mismatched Magnetic Anomalies			
Lat*	Long*	Angle, deg	Angle, km	Lat*	Long*	Angle, deg	Angle, km	Lat*	Long*	Angle, deg	Angle, km
-62.93	-119.95	1.14	20	16.27	-175.13	0.18	20	21.02	-78.69	0.18	20
-65.15	-115.02	2.10	20	14.30	-171.62	0.18	20	19.87	-76.33	0.18	20

TABLE 4. (Continued)

Skewed Fit				Mismatched Fracture Zones				Mismatched Magnetic Anomalies			
Lat*	Long*	Angle, deg	Angle, km	Lat*	Long*	Angle, deg	Angle, km	Lat*	Long*	Angle, deg	Angle, km
-53.68	115.90	0.47	20	36.32	115.90	0.18	20	0.0	-154.10	0.18	20
-51.50	120.02	0.48	20	38.47	117.46	0.18	20	1.24	-151.55	0.18	20
-44.93	111.95	0.35	20	45.07	111.95	0.18	20	0.0	-158.05	0.18	20
-45.01	142.05	0.96	20	44.99	142.05	0.18	20	0.0	-127.95	0.18	20
-43.47	141.46	1.92	40	46.53	141.36	0.36	40	0.05	-128.59	0.36	40
-43.18	141.35	1.92	40	46.82	141.22	0.36	40	0.06	-128.71	0.36	40

on their uncertainties, yield minimum resolvable relative velocities of Pacific and African hotspots in excess of 10 mm/yr for some times since Late Cretaceous time [Molnar and Stock, 1987], even allowing for uncertainties in timing of the relevant hotspot traces and the finite widths and finite durations of hotspot volcanic centers.

To compare the uncertainties in the fixed hotspot circuit with the uncertainties in the global plate circuit, the 10 mm/yr minimum relative motion between the Pacific and African hotspots can be treated as the 95% confidence level uncertainty of the fixed hotspot reconstructions of these two plates. This velocity can then be represented by a partial uncertainty rotation with a 2-sigma angle value of at least 0.090°t, where t is the time of the reconstruction in Ma. Let us overestimate the corresponding 2-sigma uncertainty in the Pacific-Africa part of the global plate circuit by taking the square root of the sum of the squares of the angle values of all partial uncertainty rotations contributing to the reconstruction (from the lists in Tables 2 and 6-9). These overestimates of the uncertainty in the Pacific-Africa reconstructions are smaller than those based on 10 mm/yr of relative motion of hotspots for all times except for anomaly 25 time, for which the uncertainties in the two methods are roughly equal. Finally, comparison of published reconstructions of the African plate over the hotspots [Duncan, 1981; Morgan, 1981, 1983] shows that for most times these reconstructions differ among

TABLE 5. Rotations and Uncertainties for Australia to Lord Howe Rise

		"Best" Pole and Angle			End Points of Plate Boundaries and Azimuths of Transform Faults				
Anomaly	Age, Ma	Lat*	Long*	Angle	Lat*	Long*	Lat*	Long*	Azimuth
25	58.94	-4.49	139.36	1.71	†	†	†	†	
28	64.71	-4.49	139.36	5.66	-33.03	159.70	-44.99	160.61	N61E
30/31	68.47	-8.70	139.34	8.97	‡	‡	‡	‡	
32	72.73	-10.63	139.33	12.30	-34.00	157.75	-42.30	161.45	N50E

See Table 2 footnotes.
* North and east are positive. Rotation angles are positive counterclockwise. Lat, latitude; Long, longitude.
† Partial uncertainty rotation axes have been rotated from anomaly 28.
‡ Partial uncertainty rotation axes have been rotated from anomaly 32.

TABLE 6. Pacific to Antarctica 'Half-Angle Stage Rotations' on Pacific Plate and Uncertainties

Anomaly		"Best" Pole and Angle			End Points of Plate Boundaries and Azimuths of Transform Faults				
Rotated	Fixed	Lat*	Long*	Angle	Lat*	Long*	Lat*	Long*	Azimuth
18	25	-47.87	107.21	3.29	†	†	†	†	
18	21	-47.87	107.21	1.44	†	†	†	†	
25	30/31	-47.87	107.21	4.21	-48.46	-161.97	-58.48	166.99	N18W
18	30/31	-47.87	107.21	7.50	†	†	†	†	

See Table 2 footnotes.
* North and east are positive. Rotation angles are positive counterclockwise. Lat, latitude; Long, longitude.
† Partial uncertainty rotation axes have been rotated from the fit of anomaly 25 to anomaly 30/31.

themselves by more than the 2-sigma uncertainties in the Pacific-Africa plate circuit [Molnar and Stock, 1987, Figure 1b]. Hence, the parameters for reconstructing Africa to the hotspots are more poorly known than the parameters for reconstructions derived from the Africa-Pacific plate circuit.

MAPS, GRAPHS, AND TABLES PRESENTED

The paleogeographic maps presented in Figures 1 and 2 show the reconstructed positions of the Pacific plate relative to fixed North America for various times. The predicted positions of selected magnetic isochrons on the Farallon and Vancouver plates have been obtained by assuming symmetric spreading; ellipses indicate uncertainties in the positions of reconstructed points.

Cumulative displacement plots (Figures 3 and 4) show the accumulated displacements of points on the Pacific and

TABLE 5. (Continued)

Skewed Fit				Mismatched Fracture Zones				Mismatched Magnetic Anomalies			
Lat*	Long*	Angle, deg	Angle, km	Lat*	Long*	Angle, deg	Angle, km	Lat*	Long*	Angle, deg	Angle, km
-40.30	157.06	1.73	20	18.19	-129.12	0.18	20	-44.09	-57.69	0.18	20
-39.01	159.84	1.73	20	22.13	-129.39	0.18	20	-42.81	-61.53	0.18	20
-39.20	157.96	2.36	20	27.16	-136.78	0.18	20	-38.76	-71.11	0.18	20
-38.16	159.49	2.36	20	30.36	-137.91	0.18	20	-37.03	-74.14	0.18	20

TABLE 6. (Continued)

Skewed Fit				Mismatched Fracture Zones				Mismatched Magnetic Anomalies			
Lat*	Long*	Angle, deg	Angle, km	Lat*	Long*	Angle, deg	Angle, km	Lat*	Long*	Angle, deg	Angle, km
-57.11	177.26	3.00	60	31.17	166.72	0.72	80	9.10	-97.73	0.72	80
-58.28	177.97	3.00	60	30.09	168.46	0.72	80	8.59	-96.53	1.08	120
-54.47	175.61	1.50	30	33.55	162.63	0.36	40	10.35	-100.42	0.36	40
-54.47	175.61	3.00	60	33.55	162.63	0.72	80	10.35	-100.42	0.72	80

Farallon/Vancouver plates through time, relative to fixed North America, by combining the positions from the different paleogeographic maps onto one map. For a given time interval the rates vary systematically with distance from the relevant pole of rotation; azimuths also vary with position, due to the curvature of the earth.

Average displacement plots (Figure 5) show displacement vectors of the adjacent oceanic plates, relative to fixed North America, as seen at points along the west coast of North America. These vectors correspond to the intervals between the magnetic polarity reversals used as bases for the paleographic maps. For each time interval the point at the specified location at the young end of the time interval is connected to its reconstructed relative position at the old end of the time interval. Uncertainty ellipses for these vectors are larger than the uncertainty ellipses on the paleogeographic maps because they incorporate the combined uncertainties of two sequential paleogeographic maps.

Note that the uncertainties in amount and direction of displacement for the points in a given time interval are not independent, because the relative spacing of the points on a rigid plate must be constant. Thus if certain portions of the uncertainty region of a given point can be reduced using independent geologic information, the corresponding portions of

TABLE 7. Rotations and Uncertainties for Antarctica to India

Anomaly	"Best" Pole and Angle			End Points of Plate Boundaries and Azimuths of Transform Faults				
Rotated	Lat*	Long*	Angle	Lat*	Long*	Lat*	Long*	Azimuth
5 ‡	26.09	20.48	5.60					
6 ‡	18.47	29.56	11.37					
13 ‡	13.42	30.52	20.51					
18	15.61	29.26	23.94	...	...	...	...	...
20	16.44	28.78	25.57	-17.50	78.00	-22.00	84.00	N2E
21	16.36	23.96	27.99	...	...	...	...	...
23	16.19	19.38	30.94	-14.00	78.20	-18.25	84.10	N2E
25	16.95	12.60	35.51	-11.10	78.10	-12.30	80.00	N2E
28	12.05	13.64	45.62	-6.50	77.70	-11.05	83.30	N2E
30/31	11.76	11.53	50.66	-4.15	77.30	-8.55	83.25	N2E
33(young)	11.83	10.08	55.55	-2.30	77.28	-5.90	82.85	N2E
33(old)	11.72	9.31	59.56	-1.25	80.32	...	...	N2E
34	11.79	8.57	62.25	0.00	80.33	...	...	N2E

From Molnar et al. [1988].
* North and east are positive. Rotation angles are positive counterclockwise. Lat, latitude; Long, longitude.
† Values in parentheses give overlap or underlap in km of end points of the plate boundary
‡ Calculated from other boundaries in the Indian Ocean.
§ Mismatch of 100 km at 5 degrees from pole.

TABLE 8. Rotations and Uncertainties for India to Africa

	"Best" Pole and Angle			End Points of Plate Boundaries and Azimuths of Transform Faults				
Anomaly	Lat*	Long*	Angle	Lat*	Long*	Lat*	Long*	Azimuth
5	25.88	37.94	-5.06	0.75	59.60	-22.40	67.00	N57E
6	17.73	44.44	-10.78	-25.05	65.65	...	...	N58E
13	14.57	46.75	-19.20	-17.95	61.80	-37.10	69.35	N61E
18	17.46	46.85	-22.23	...	...	...	...	...
20	18.54	46.89	-23.82	6.00	57.00	-24.00	60.00	N34E
21	19.67	42.41	-25.11	...	...	...	...	...
23	20.70	37.76	-26.74	3.95	55.95	-26.15	58.45	N33E
25	22.79	29.38	-29.93	1.35	55.85	-27.57	55.50	N34E
28	18.29	26.56	-39.88	-27.97	51.11	...	...	N39E
30/31 ‖	18.45	23.47	-44.14	...	...	...	...	...
33(old)‖	20.32	21.39	-51.30	...	...	...	...	...
34 ‖	23.36	19.57	-51.54	...	...	...	...	...

From Molnar et al. [1988].
* North and east are positive. Rotation angles are positive counterclockwise. Lat, latitude; Long, longitude.
† Value in parentheses give overlap or underlap in kilometers of of endpoints of the plate boundary.
‡ Mismatch of 1 degree (111.4 km) at 30 degrees from pole.
§ Mismatch of 2 degrees (222.8 km) at 28 degrees from pole.
‖ Calculated from other boundaries in the Indian Ocean.

TABLE 7. (Continued)

Skewed Fit				Mismatched Fracture Zones				Mismatched Magnetic Anomalies			
Lat*	Long*	Angle, deg	Angle,† km	Lat*	Long*	Angle, deg	Angle, km	Lat*	Long*	Angle, deg	Angle, km
-20.45	80.46	7.13	794	69.42	87.23	0.36	40	2.22	-8.71	0.90	100
-19.78	80.96	7.13	794(50)	70.12	86.85	0.36	40	1.88	-8.36	0.90	100
-18.17	81.00	7.13	794	71.70	87.83	0.36	40	2.03	-8.33	0.90	100
-16.15	81.12	2.91	324(20)	73.73	88.28	0.36	40	1.92	-8.32	0.13	15
-11.70	78.95	7.01	781(15)	78.13	88.72	0.36	40	1.96	-10.64	0.27	30
-8.78	80.48	2.16	240(15)	81.00	93.36	0.36	40	1.98	-9.21	0.13	15
-6.35	80.26	2.10	234(15)	83.34	97.78	0.36	40	1.99	-9.52	0.11	12
-4.10	80.06	3.11	346(20)	85.44	106.09	0.36	40	1.99	-9.80	0.13	15
-1.25	80.32	10.30	1147 §	87.64	138.33	0.36	40	2.00	-9.64	0.36	40
0.00	80.33	10.30	1147 §	88.00	170.33	0.36	40	2.00	-9.67	0.36	40

TABLE 8. (Continued)

Skewed Fit				Mismatched Fracture Zones				Mismatched Magnetic Anomalies			
Lat*	Long*	Angle, deg	Angle, † km	Lat*	Long*	Angle, deg	Angle, km	Lat*	Long*	Angle, deg	Angle, km
-10.84	63.16	0.64	71 (15)	32.34	146.20	0.18	20	55.46	-10.69	0.09	10
-25.05	65.65	2.00‡	223 ‡	28.69	140.83	0.27	30	50.20	9.77	0.27	30
-27.57	65.24	0.77	85 (15)	25.45	140.85	0.27	30	50.83	15.10	0.13	15
-8.92	58.97	2.76	308	56.61	135.72	0.36	40	32.90	-25.20	0.90	100
-9.00	58.44	2.76	308 (80)	54.97	135.38	0.36	40	33.53	-25.54	0.90	100
-9.91	57.79	2.76	308	54.50	133.60	0.36	40	33.69	-25.53	0.90	100
-11.10	57.13	0.69	77 (20)	55.38	130.62	0.27	30	32.31	-25.74	0.13	15
-13.11	55.69	1.08	120 (30)	53.85	127.10	0.27	30	33.00	-25.61	0.18	20
-27.97	51.11	4.26§	475 §	43.34	111.03	0.36	40	33.77	-18.09	0.36	40

the uncertainty regions for other points on that plate must also be reduced.

Selection of a magnetic anomaly time scale allows the average relative velocities to be calculated by dividing the displacements by the appropriate time intervals (Tables 15 and 16). Uncertainties in these velocities are also derived by dividing the spatial uncertainty in the displacement by the time interval on the DNAG time scale; no additional uncertainty in the length of the time interval is included. These velocities can be plotted together to show the relative plate motion at one point through time, as vectors (Figure 6). These may also be plotted as

TABLE 9. Rotations and Uncertainties for Antarctica to Africa

	"Best" Pole and Angle			End Points of Plate Boundaries and Azimuths of Transform Faults				
Anomaly	Lat*	Long*	Angle	Lat*	Long*	Lat*	Long*	Azimuth
5	11.72	-43.84	1.55	-44.00	36.59	-26.58	66.60	N5E
6	11.72	-43.84	2.79	-43.48	36.76	-29.11	59.60	N8E
7 ‡	10.00	-41.50	3.84					
10 ‡	9.25	-40.49	4.59					
13	8.57	-39.59	5.58	-42.17	37.54	-34.90	51.00	N10E
18 ‡	8.79	-40.72	6.95					
20	8.86	-41.12	7.61	-41.27	38.23	-28.70	57.65	N7E
21 ‡	8.09	-39.28	8.65					
23 §	7.40	-37.66	9.85					
25 §	6.43	-39.15	10.94					
28 §	2.76	-40.26	11.63					
30/31 ‡	2.22	-40.74	12.50					
33	0.75	-42.06	15.71	-45.24	21.42	-35.90	41.55	N2E
34	-5.03	-39.12	18.24	-44.46	23.01	-34.76	41.19	N5E

From Molnar et al. [1988].
* North and east are positive. Rotation angles are positive counterclockwise. Lat, latitude; Long, longitude.
† Values in parentheses give overlap or underlap in kilometers of endpoints of the plate boundary.
‡ Pole positions, angles, and partial uncertainty rotations interpolated between those for neighboring anomalies.
§ Pole positions and angles calculated from those for the other segments of the Indian Ocean.

bar graphs of speed and azimuth with respect to time (Figure 7) but in this case some information is lost because the uncertainties in speed and azimuth are correlated.

DISCUSSION

Pacific-North America Interactions

General history of relative motion. Between the times of anomalies 30/31 and 18 (68 to 42 Ma) the Pacific plate moved approximately north relative to fixed North America (Figure 4; Table 15). Slight differences in the azimuth of approach of the Pacific plate for smaller intervals within this period cannot be resolved because they are smaller than the average 50°-70° uncertainty in this azimuth. The best fit average speeds of the Pacific plate adjacent to North America decreased by a factor of two in this time interval, but these decreases were smaller than the uncertainties in the calculated speeds. The average speed for the entire interval between anomalies 30/31 and 18 (68 to 42 Ma), however, is constrained by the cumulative displacements to be 51±6 mm/yr and 50±8 mm/yr for the two points listed in Table 15.

After 42 Ma the Pacific plate moved more northwesterly with respect to fixed North America. Resolvable changes in both speed and direction of the Pacific plate with respect to North America occurred. For instance, the average rate of Pacific-North America motion since anomaly 5 time (10.6 Ma) is demonstrably faster than the rate in the interval between anomalies 5 and 6 (19.9-10.6 Ma; Table 15). A change in average direction is required since the time of anomaly 6 (Figure 4), but it could have occurred either before or after

TABLE 9. (Continued)

Skewed Fit				Mismatched Fracture Zones				Mismatched Magnetic Anomalies			
Lat*	Long*	Angle, deg	Angle,† km	Lat*	Long*	Angle, deg	Angle, km	Lat*	Long*	Angle, deg	Angle, km
-36.22	53.25	0.52	58(15)	53.48	61.67	0.18	20	4.03	-33.79	0.09	10
-36.84	49.25	0.67	75(15)	52.42	62.44	0.18	20	6.39	-35.93	0.11	12
-36.31	49.34	0.84	93	52.94	62.59	0.22	25	6.38	-35.94	0.13	15
-39.21	44.50	2.01	224	49.71	60.25	0.22	25	7.82	-39.07	0.22	25
-38.72	44.62	1.61	180(20)	50.21	60.36	0.18	20	7.79	-39.09	0.18	20
-35.69	48.66	1.61	180	53.72	60.21	0.34	38	5.65	-37.25	0.22	25
-35.37	48.70	1.02	114(20)	54.03	60.68	0.27	30	5.70	-37.23	0.18	20
-34.85	48.83	1.53	170	54.57	60.67	0.40	45	5.59	-37.25	0.27	30
-42.59	32.06	2.32	258	47.35	35.66	0.72	80	1.79	-56.30	0.27	30
-41.01	32.19	1.16	129(20)	48.95	35.24	0.36	40	1.51	-56.50	0.13	15
-39.96	32.75	1.22	135(20)	49.78	40.51	0.36	40	3.83	-54.03	0.13	15

anomaly 5 time [Stock and Hodges, 1988].

The largest changes in the relative velocity of the Pacific and North America plates occurred between the times of anomalies 21 and 13 (50 to 36 Ma). During this interval the approach azimuth rotated counterclockwise (from north to NW), and the relative speed decreased. These two changes are linked to changes in two different parts of the plate circuit and may not have been simultaneous.

The change in direction is primarily linked to a major change in Pacific-Antarctica spreading direction that occurred in the southwest Pacific during this interval [Stock and Molnar, 1987]. The uncertainties in the reconstructions, which correspond only to selected times, do not allow us to constrain more precisely the time of the change in motion of the Pacific plate relative to North America. In the best fit reconstructions it occurs near anomaly 18 time (42 Ma), approximately the age of the Hawaiian-Emperor bend.

The reduction in Pacific-North America relative speed appears to have started closer to anomaly 21 time, 50 Ma, than to anomaly 18 time, 42 Ma. It is linked primarily to a major change in direction of spreading between Africa and North America at about anomaly 21 time [Klitgord and Schouten, 1986]. The con sequent reduction of Pacific-North America relative speed is reflected in the calculated motion of the Farallon and Vancouver plates with respect to North America (see next section). A major change in Pacific-North America motion at anomaly 21 time was not identified in various earlier studies based on the assumption of fixed hotspots [e.g., Engebretson et al., 1985, Figure A1], either because individual reconstruction parameters were not determined at close enough time intervals or because of difficulties in determining the motion of North America directly over the hotspots. For example, Engebretson et al. [1985] used no independent Africa-North America reconstruction parameters for times between anomalies 13 and 30/31. In either the global plate circuit or the hotspot circuit the inclusion of this change in central Atlantic spreading near anomaly 21 time has a profound effect on the Pacific-North America reconstructions.

Initiation of the Mendocino and Rivera triple junctions. The time and position at which the Pacific-Farallon ridge reached the trench west of North America, initiating the triple junction of the Pacific, Farallon, and North America plates, is important for understanding the development of strike-slip fault systems along the Pacific-North America plate

TABLE 10. Rotations and Uncertainties for the Central Atlantic Ocean (Africa to North America)

	"Best" Pole and Angle			End Points of Plate Boundaries and Azimuths of Transform Faults				
Anomaly	Lat*	Long*	Angle	Lat*	Long*	Lat*	Long*	Azimuth
5 † (center)	79.08	77.95	-2.41	22.54	-46.46	37.88	-32.68	100
5 ‡ (old edge)	79.53	71.47	-2.66					
6	79.57	37.84	-5.29	23.66	-47.89	37.48	-35.52	104
13	76.41	7.12	-9.81	24.44	-49.93	37.53	-37.16	105
18 §	75.36	-0.28	-12.44					
20 §	74.96	-2.54	-13.68					
21	74.51	-4.83	-15.32	21.80	-52.70	33.52	-46.30	098
25	80.60	-0.50	-18.07	21.90	-54.65	33.77	-48.23	085
30	82.51	-0.63	-20.96	17.33	-56.75	37.30	-44.18	087
30/31 §	82.28	-2.61	-21.33					
32	81.35	-9.15	-22.87	17.30	-57.98	36.68	-45.15	110
33 young	80.76	-11.76	-23.91	17.35	-58.35	37.32	-45.13	112
33 old	78.30	-18.35	-27.06	17.35	-59.95	36.12	-47.05	110
34	76.55	-20.73	-29.60	18.05	-60.92	37.60	-46.28	115

Source of best pole and angle for anomalies 5 (center), 6, 13, 25, 30, 32, 33y, 33o, and 34 is Klitgord and Schouten [1986]. Source of all other calculations is this paper.

* North and east are positive. Rotation angles are positive counterclockwise. Lat, latitude; Long, longitude.

† Middle of anomaly 5 is 9.67 Ma on the DNAG timescale [Berggren et al., 1985].

‡ Best pole and angle interpolated (by time scale) between values for neighboring anomalies; partial uncertainty rotations rotated from anomaly 5 (center).

§ Pole positions, angles, and partial uncertainty rotations interpolated between those of neighboring anomalies.

boundary. Pacific-Farallon-North America triple junctions developed in two places at two different times: (1) at the north end of the Farallon-Kula ridge, after Kula-Pacific spreading stopped or after a ridge jump transferred part of the Kula plate to the Pacific plate [e.g., Lonsdale, 1988]; and (2) further south, when a central section of the Pacific-Farallon ridge, south of the Mendocino fracture zone, approached the Farallon-North America subduction zone. Here we discuss the southern location, which later developed into the Mendocino and Rivera triple junctions.

The time of contact between the Pacific-Farallon ridge and the North America plate can be constrained more accurately by study of the remaining Pacific-Farallon magnetic anomalies on the Pacific plate [Atwater, 1970] than by global plate reconstructions. For instance, within the uncertainties for positions of the Pacific-Farallon ridge, the reconstruction for the time of anomaly 13 (36 Ma, Figure 2f) includes an overlap of the ridge with the North American coast. This age of initiation of the Pacific-North America boundary is ruled out, however, by the presence offshore of a complete, continuous set of lineations for anomalies 18 to 10 (42 to 30 Ma),

TABLE 10. (Continued)

Skewed Fit				Mismatched Fracture Zones				Mismatched Magnetic Anomalies			
Lat*	Long*	Angle, deg	Angle, km	Lat*	Long*	Angle, deg	Angle, km	Lat*	Long*	Angle, deg	Angle, km
30.40	-40.11	0.32	36	-8.61	44.79	0.09	10	58.15	120.68	0.036	4
30.42	-40.23	0.32	36	-8.63	44.66	0.09	10	58.12	120.54	0.036	4
30.72	-42.15	0.41	46	-12.00	40.59	0.09	10	56.53	111.83	0.036	4
31.13	-43.99	0.42	47	-12.80	38.12	0.09	10	55.77	108.61	0.036	4
31.30	-45.00	0.63	70	-13.18	36.81	0.13	15	55.43	106.95	0.072	8
27.57	-49.02	0.79	88	-6.85	37.39	0.17	19	61.45	114.65	0.09	10
27.70	-49.67	0.63	71	-7.08	36.59	0.13	15	61.26	113.51	0.045	5
27.87	-51.62	0.71	79	4.42	40.72	0.09	10	61.72	138.98	0.045	5
27.45	-51.04	0.32	35	2.66	40.34	0.09	10	62.40	135.45	0.054	6
27.46	-51.18	0.48	53	2.58	40.16	0.13	15	62.40	135.12	0.09	10
27.13	-52.13	0.37	41	-17.72	28.45	0.09	10	56.75	89.27	0.045	5
27.49	-52.35	0.31	35	-19.41	27.09	0.13	15	55.34	86.45	0.045	5
26.88	-54.04	0.33	37	-17.76	26.62	0.13	15	56.95	87.13	0.045	5
28.02	-54.27	0.35	39	-21.91	23.37	0.13	15	53.14	80.94	0.045	5

formed by Pacific-Farallon spreading during this interval [Atwater, 1970; Atwater and Menard, 1970]. The clockwise rotation of the lineations of anomalies 9 and younger between the Pioneer and Murray fracture zones indicates that this part of the Farallon plate was close enough to North America to break up just after anomaly 10 time, at approximately 28.5 Ma [Atwater, 1970; Menard, 1978; J. Severinghaus and T. Atwater, manuscript in preparation, 1988]. This breakup may have preceded the time of direct contact between the Pacific and North America plates; Atwater [1988] estimates that the direct contact occurred sometime between 28 and 25 Ma. The triple junctions would have initiated at the intersection of the Pioneer fracture zone with the edge of the North America plate. At 28.5 Ma, relative to fixed North America, this would have been at latitude 31.3°N ± 130 km, west of northernmost Sonora, and approximately offshore from Point Arguello, California, with the Gulf of California closed by the 5.5 Ma reconstruction. If the triple junction did not initiate until a younger time, it would have been further north relative to western North America.

Path of the northern (Mendocino) triple junction. Because the triple junction is now formed by the intersection of the Mendocino fracture zone, rather than the Pioneer fracture zone, with the San Andreas fault, the triple junction must have jumped north more recently, in Miocene time, as the ridge between the Pioneer and Mendocino fracture zones approached the trench. The youngest clearly identified magnetic anomaly between these two fracture zones is anomaly 8 [Atwater, 1970], which is parallel to anomaly 8 lineations extending north into the Gulf of Alaska; thus if the triple junction formed before anomaly 8 time, it would have jumped northward sometime after anomaly 8 time (27 Ma). Our analysis follows the past position of the northern Pacific-Farallon-North America triple junction as the position of the Pioneer fracture zone along the coast from perhaps 28.5 Ma to at least 27 Ma and the Mendocino fracture zone thereafter. If the triple junction did not initiate until 25 Ma, then the Pacific-North America displacement in the interval prior to 25 Ma would have been accommodated by interactions with the intervening

TABLE 11a. Best fit Rotations for Pacific-Farallon Magnetic Anomalies

Anomaly Rotated	Anomaly Fixed	Lat*	Long*	Angle
13	18 ‡	80.71°N	101.84°E	-4.10°
13	18 †	80.71°N	101.84°E	-3.95°
13	21	82.06°N	119.39°E	-8.39°
13	25	75.91°N	81.36°E	-12.43°
13	30/31	74.52°N	81.28°E	-16.10°
13	32	74.32°N	80.77°E	-17.30°
18 ‡	21	82.26°N	140.00°E	-4.30°
18 †	21	82.28°N	138.57°E	-4.45°
18 ‡	25	73.36°N	74.85°E	-8.37°
18 ‡	30/31	72.34°N	76.60°E	-12.05°
18 ‡	32	72.29°N	76.35°E	-13.25°
21	25	59.77°N	59.09°E	-4.36°
21	30/31	64.86°N	66.00°E	-8.00°
21	32	65.81°N	66.61°E	-9.19°
25	30/31	69.87°N	79.17°E	-3.69°
25	32	70.37°N	77.89°E	-4.89°
30/31	32	71.89°N	73.76°E	-1.20°

From Rosa and Molnar [1988].
* Lat, latitude; Long, longitude.
† 42.01 Ma on DNAG time scale (see Table 1).
‡ 42.26 Ma on DNAG time scale [from Rosa and Molnar, 1988].

subducting plate and not along a Pacific-North America strike-slip boundary.

The uncertainty in the past positions of points on the Pacific plate near the eastern end of the Mendocino fracture zone, relative to North America, are ±50 km at 5.5 Ma, ±50 km at anomaly 5 time, ±60 km at anomaly 6 time, ±90 km at anomaly 7 time, and ±175 km at anomaly 10 time. These are distances resolved parallel to the present coastline after closure of the San Andreas fault and Gulf of California by the 5.5 Ma reconstruction. For the average rate of motion of the Pacific plate parallel to the North American coastline at this latitude (approximately 40 mm/yr during Neogene time) these correspond to uncertainties ranging from ±1 m.y. to ±4 m.y. in the time that these points passed specific locations on the coast. These uncertainties ignore displacements of small crustal blocks and changes in the shape of the coastline [e.g., Luyendyk et al., 1985].

Total displacement parallel to the San Andreas fault system. The plate reconstructions provide bounds on the total relative motion that should have occurred across the Pacific-North America plate boundary after these two plates came into contact (Figure 3; Table 16). Hence they provide bounds on measured geologic displacement and/or strain deduced from palinspastic reconstructions of fault systems of the Pacific-North America margin. To interpret these bounds, one must remember that the length of the Pacific-North America boundary has increased with time, that different faults within the plate boundary zone have been active at different times, and that slices of crust along the plate boundary zone may have been transferred back and forth from the Pacific to the North America plates in this process.

For example, the 23.5 Ma Neenach Volcanics crop out in the westernmost Mojave Desert, east of the San Andreas

TABLE 11b. Corresponding Partial Uncertainty Rotations

Rotation	Skewed Misfit	Mismatched Magnetic Anomalies	Mismatched Fracture Zones
13-18 *†	33.46°N	55.24°S	8.33°N
	131.55°W	113.81°W	36.00°W
	0.360°	0.180°	0.180°
18-21 *†	33.50°N	55.08°S	8.74°N
	135.62°W	117.06°W	39.78°W
	0.360°	0.180°	0.180°
21-25	33.75°N	53.78°S	11.60°N
	141.00°W	116.83°W	43.11°W
	0.360°	0.180°	0.180°
25-30/31	33.78°N	53.75°S	11.60°N
	145.23°W	121.08°W	47.34°W
	0.360°	0.180°	0.180°
30/31-32	41.42° N	45.15°S	14.13°N
	154.01°W	126.52°W	51.18°W
	1.21°	0.180°	0.180°

* 42.01 Ma on DNAG time scale (see Table 1).
† 42.26 Ma on DNAG time scale [from Rosa and Molnar, 1988].

TABLE 12a. Best Fit Rotations of Pacific-Vancouver Magnetic Anomalies Younger Than Anomaly 21, North of the Pioneer Fracture Zone

Anomaly Rotated	Anomaly Fixed	Lat*	Long*	Angle
13	18 ‡	78.00°N	140.00°W	-5.55°
13	18 †	78.00°N	140.00°W	-5.33°
13	21	76.70°N	139.40°W	-11.12°
18 ‡	21	75.40°N	139.40°W	-5.57°
18 †	21	75.50°N	139.40°W	-5.79°
21	25	83.36°N	160.00°W	-6.06°
18 †	25	79.58°N	141.22°W	-11.61°
13	25	79.06°N	145.02°W	-17.15°

All rotations are from Rosa and Molnar [1988], except for A25-A21, which was spatially extrapolated from the A18-A21 pole in this table (for A21-A24) and the A21-A25 pole in Table 11 (for A24-A25).

* Lat, latitude; Long, longitude.

† 42.01 Ma on DNAG time scale (see Table 1).

‡ 42.26 Ma on DNAG time scale [from Rosa and Molnar, 1988].

fault. At this latitude on the North American side of the plate boundary zone, 900 ± 100 km of strike-slip displacement should have occurred since the passage of the Mendocino triple junction at approximately 20 Ma. (Note that the triple junction would have initiated south of here, so the accumulated Pacific-North America displacement in the plate boundary zone is less here than it would be further south.) The Pinnacles volcanics, the offset equivalents of the Neenach volcanics west of the San Andreas fault on the Pacific plate, are found only 315 km to the north [Matthews, 1973, 1976]. Thus the Pinnacles-Neenach outcrops do not span the entire plate boundary zone, and the 315 km of offset is only part of the total strike-slip displacement integrated across the plate boundary zone at the latitude of the Neenach volcanics, relative to fixed North America.

The additional 585 ± 100 km of displacement must have occurred on structures west of the San Andreas fault and north of the Pinnacles on the Pacific plate and/or on structures east of the San Andreas fault and south of the Neenach volcanics on the North America plate. Possible locations of this motion include the San Gregorio fault system (with 150 km of offset of Upper Miocene rocks [Clark et al., 1984]), other right-lateral faults to the west or offshore, and the southern Basin and Range province. In general, at any point along the plate boundary the total plate boundary displacement may be partitioned among offshore faults, older strands of the San Andreas system, and deformation between the San Andreas and the Colorado Plateau [Atwater, 1970; Atwater and Molnar, 1973; Graham and Dickinson, 1978].

On the North American side of the San Andreas fault system the accumulated strike-slip displacement across the Pacific-North America plate boundary decreases northwestward because of the northwestward migration of the Mendocino triple junction relative to the North America plate. On the Pacific side of the San Andreas fault system the accumulated strike-slip displacement relative to North America decreases southeastward because of the southeastward migration of the Rivera triple junction relative to the Pacific plate. Separation of the two triple

TABLE 12b. Corresponding Partial Uncertainty Rotations

Rotation	Skewed Misfit	Mismatched Magnetic Anomalies	Mismatched Fracture Zones
13-18 *†	48.99°N 148.31°W 1.31°	40.99°S 146.32°W 0.180°	0.98°N 57.17°W 0.180°
18*†-21	48.13°N 143.93°W 1.60°	41.86°S 141.92°W 0.180°	1.00°N 52.81°W 0.180°
21-25	48.25°N 138.29°W 1.60°	41.72°S 135.55°W 0.180°	1.36°N 46.76°W 0.180°

Rotations 13-18 and 18-21 from Rosa and Molnar [1988]. Rotations 21-25 from this paper.

* 42.01 Ma on DNAG time scale (see Table 1).

† 42.26 Ma on DNAG time scale [from Rosa and Molnar, 1988].

TABLE 13a. Best Fit Rotations for Pacific-Kula Magnetic Anomalies

Anomaly Rotated	Anomaly Fixed	Lat*	Long*	Angle
25	30/31	27.50°N	126.25°E	-3.10°
25	32	27.50°N	126.25°E	-4.60°
30/31	32	27.50°N	126.25°E	-1.50°

* Lat, latitude; Long, longitude.
From Rosa and Molnar [1988].

junctions results in juxtaposition of rocks with very different strain histories within the plate boundary zone. The eastern edge of the Pacific plate just south of the Mendocino triple junction should have undergone about 1200 km of strike-slip motion since 27 Ma, but the part of North America immediately to the east has undergone shear strain only in the past few million years.

The unacceptable overlap at 25-35 Ma; Extension in the Basin and Range, or deformation in Antarctica? In the reconstructions for the times of anomalies 7 to 13 (Figures 2d-2f), oceanic crust of the Pacific plate overlaps North American continental crust after closure of the Gulf of California by the 5.5 Ma reconstruction. The amounts of overlap, here measured by the distance from the reconstructed Pacific-Farallon ridge to the 1000 fm (1829 m) isobath, reach 260±75 km at the time of anomaly 7, 340±200 km at the time of anomaly 10, and 150±75 km at the time of anomaly 13. These values are minimum constraints on the total overlap, which also includes an unknown width of oceanic crust of the Farallon plate, lying east of the Pacific-Farallon ridge but west of the North America plate at these times. The amount of overlap farther north cannot be constrained by the reconstructions because the spreading center was farther offshore, and Farallon (Vancouver) plate crust that might indicate overlap has been subducted.

These overlaps suggest that deformation, in addition to that attributed to the opening of the Gulf of California, has occurred within at least one of the "rigid" plates. This unacceptable overlap in the reconstructions was noted by previous workers [Atwater, 1970; Atwater and Molnar, 1973; Engebretson et al., 1985], who suggested that it might be due to Tertiary extension of western North America. Increasing evidence of several hundred kilometers of crustal extension in parts of the Basin and Range province [e.g., Wernicke et al., 1988] is consistent with this possibility. If all of this overlap were due to extension within western North America, and the other plates in the plate circuit had behaved rigidly, this overlap implies a minimum of 340±200 km of extension perpendicular to the coast (azimuth N60°E) at the latitude of northern Sonora (30°N) since the time of anomaly 10 (30 Ma). Note that if extension at this latitude were not oriented parallel to N60°E, a greater amount of extension would be implied. For example, if the geologic extension direction were N70°W (similar to that documented further north by Wernicke et al. [1988]), 500±250 km of extension would be indicated (Figure 8). Unfortunately, neither the amount nor the direction of crustal extension at 30°N is known.

Because the reconstructions showing the overlap are based on a global plate circuit, other areas in the circuit should also be examined for possible nonrigid behavior. East Africa is sometimes considered to be a separate plate, the Somali plate, moving very slowly away from the rest of Africa with an angular velocity of 0.06°/m.y. [e.g., McKenzie et al., 1970; Chase, 1978]. Our reconstructions for anomaly 18 to the present use ridges bounding Africa on the northwest and south to southeast sides, not near the Somali

TABLE 13b. Corresponding Partial Uncertainty Rotations

Rotation	Skewed Misfit	Mismatched Magnetic Anomalies	Mismatched Fracture Zones
25-30/31	48.66°N	0.00°N	41.34°N
	171.25°W	81.25°W	8.75°E
	1.750°	0.180°	0.180°
30/31-32	47.26°N	0.00°N	42.74°N
	169.50°W	79.50°W	10.49°E
	2.73°	0.360°	0.250°

From Rosa and Molnar [1988].

TABLE 14a. Finite rotations of the Pacific Plate to North America

Magnetic Anomaly	Time, Ma	Source (Other Than Tables)	Latitude	Longitude	Angle
3	5.5	instantaneous rates	48.62°N	75.15°W	4.70°
5	10.59		55.50°N	68.41°W	8.46°
6	19.90		52.15°N	74.82°W	12.63°
7	25.8	interpolations	55.15°N	71.50°W	16.06°
10	30.0	interpolations	56.56°N	70.05°W	18.53°
13	35.58		57.93°N	68.91°W	21.82°
18	42.01		57.84°N	68.72°W	24.55°
21	49.55		52.13°N	70.89°W	25.89°
25	58.94		42.74°N	70.05°W	29.52°
30/31	68.47		37.51°N	73.35°W	36.59°

Numbers obtained by summing the appropriate rotations from Tables 2-10. The sources of rotations not derived from Tables 2-10 are specified. See text for discussion.

plate, and presumably have not been affected by the small amount of Somali plate motion. The oceanic part of the India plate is deforming internally south of India [e.g., Stein and Okal, 1978; Wiens et al., 1985], but the India plate is not involved in our reconstructions for anomalies 18 and younger. Our anomaly 25 reconstruction does involve the India plate and the Somali margin of Africa, and so for this time a small amount (<100 km) of internal deformation in these two plates may need to be incorporated in the reconstructions.

Internal deformation may have occurred within West Antarctica [Dalziel, 1982], but the timing and amount of motion is not well constrained. Relative motion of East and West Antarctica may also have occurred during the Cenozoic era [e.g., Hamilton, 1967]. Fitzgerald et al. [1987] suggest that a maximum of 200 km of extension occurred across the Transantarctic rift system (between East and West Antarctica) during this time. As neither the position of the pole of rotation for this motion, nor the timing, is well constrained, the effect of this motion on the Pacific-North America reconstructions cannot be quantitatively evaluated. We estimated the effect of such rifting on the overlap by arbitrarily selecting three representative

TABLE 14b. Order of Component Rotations for Sample Reconstruction Requiring the Use of a Half-Angle ("Stage") Rotation on One Plate: Anomaly 21, Pacific to North America

Order	Component Rotation	Latitude	Longitude	Angle
1	A21 to A18 on Pacific plate (with full angle, not half angle)	47.87°S	107.21°E	-2.88°
2	Pacific to Antarctica anomaly 18 time	75.08°N	51.25°W	32.56°
3	Antarctica to Africa anomaly 21 time	8.09°N	39.28°W	8.65°
4	Africa to North America anomaly 21 time	74.51°S	175.17°E	15.32°

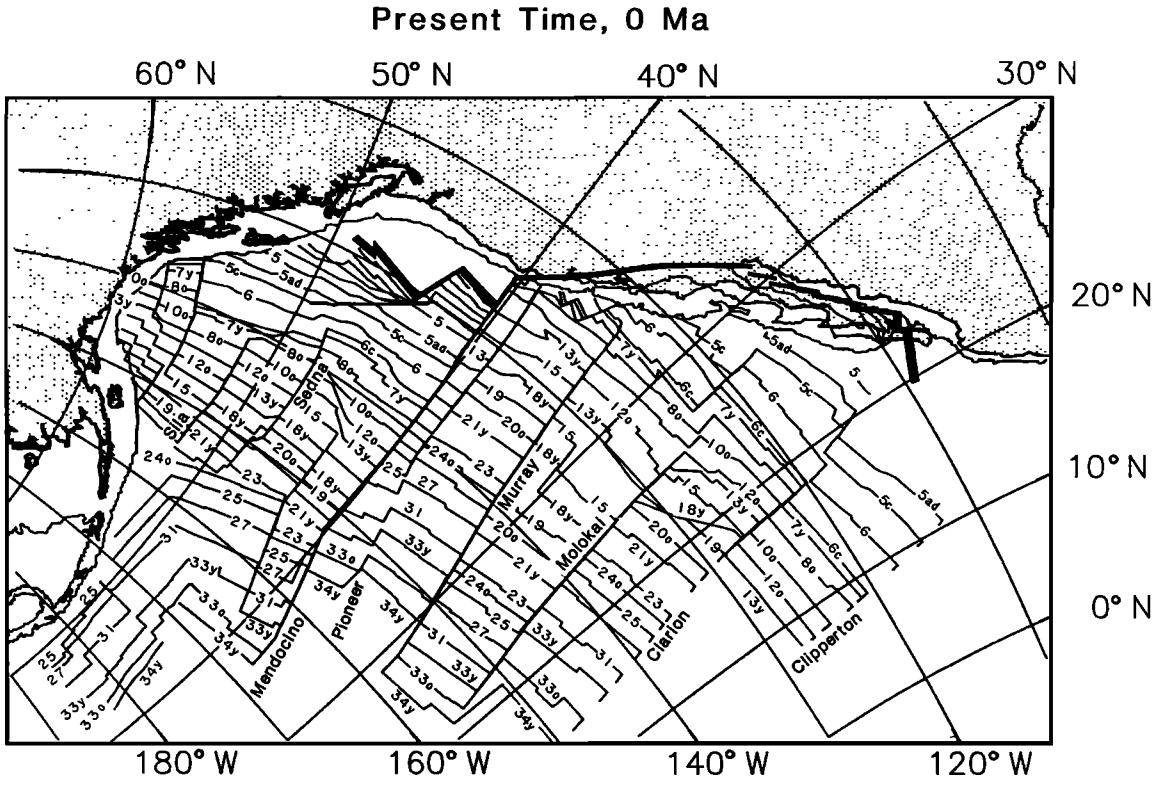

Fig. 1. Present North American coast, 1000 fm (1829 m) contour and selected magnetic isochrons [from Atwater and Severinghaus, 1988] on the Pacific plate. Map is an oblique Mercator projection about 52.15°N, 74.82°W, the anomaly 6 finite pole for Pacific-North America reconstruction. Spreading ridges are heavy black lines; strike-slip and convergent boundaries are medium black lines. Ages of isochrons on the DNAG time scale [Berggren et al., 1985; Kent and Gradstein, 1985] are as follows: 34y (young edge), 84.00 Ma; 33o (old edge), 80.17 Ma; 33y, 74.30 Ma; 31, 68.96 Ma; 27, 63.28 Ma; 25, 58.94 Ma; 24o, 56.14 Ma; 23, 54.29 Ma; 21y, 48.75 Ma; 20o, 46.17 Ma; 19, 43.83 Ma; 18, 41.29 Ma; 15, 38.10 Ma; 13y, 35.29 Ma; 12o, 32.90 Ma; 10o, 30.33 Ma; 8o, 27.74 Ma; 7y, 25.67 Ma; 6c, 24.12 Ma; 6 (old edge) 20.45 Ma; 5c (old edge) 16.89 Ma; 5ad, 14.43 Ma; 5 (old edge) 10.42 Ma; 3a (old edge), 5.89 Ma.

rotations to produce 200 km of motion of West Antarctica toward East Antarctica, perpendicular to the Transantarctic rift system: rotations about three poles on the 150°E meridian at 0°N, 45°N, and 45°S. Inclusion of any of these rotations in the Pacific-North America plate circuit for anomaly 10 time results in point positions south of, and outside the uncertainty regions of, the positions derived by assuming no relative motion between East and West Antarctica (Figure 8). The three rotations chosen to close the Transantarctic rift do reduce the overlap of the Pacific plate with western North America by significant and varying amounts, leaving open the possibility that nonrigid deformation within western North America and/or within Antarctica might have been of the right order and sense to cause the overlap problem in the reconstructions. However, fixed hotspot reconstructions (which completely bypass Antarctica and should be unaffected by deformation there) yield even more overlap than does the global plate circuit (Figure 8). This suggests that inter-Antarctica deformation cannot be the cause of the apparent overlap.

Evidence from the Pacific-Antarctica-Australia-Lord Howe Rise plate circuit suggests that inter-Antarctic deformation may affect the plate circuit principally between the times of anomalies 13 and 6 and that its total effect in the southwest Pacific reconstructions is small (less

than a few hundred kilometers [Stock and Molnar, 1987]). Thus we applied two additional tests of the three rotations used to close the Transantarctic rift system, using the anomaly 13 reconstructions. First, two of these three rotations reduce (by 150 and 300 km) but do not eliminate the discrepancy between the predicted and actual positions of the Hawaiian hotspot at anomaly 13 time [see Molnar and Stock, 1987]. Second, even if all of the Transantarctic rifting occurred between anomaly 6 and anomaly 13 time, the reconstructions still require 200 ± 100 km of strike-slip motion parallel to the Alpine fault system (accompanied by possibly up to an equal amount of either compression or extension) across the Pacific-Australia plate boundary in New Zealand during this interval. If these rotations bound the range of acceptable descriptions of Antarctic rifting, they do not eliminate what might be discrepancies between the geologic history of New Zealand and plate reconstructions [see Kamp and Fitzgerald, 1987].

One major difference between our reconstructions, and some based on fixed hotspots, is the amount of displacement of the Pacific plate relative to North America between the times of anomalies 6 and 5. For a point close to the Mendocino triple junction our reconstructions yield an average velocity of approximately 26±10 mm/yr during this period (Figure 5b; Table 16), slower than previously found by assuming fixed hotspots [e.g., Engebretson et al., 1985]. (Note that the velocities listed in Table 15 are larger for this interval because the points studied in Table 15 are further from the stage pole for Pacific-North America motion for this interval.) The fixed hotspot circuit for 30 Ma reconstructs a point further southeast along the boundary than does the global plate circuit (Figure 8), implying greater cumulative motion along the Pacific-North America boundary. Part of the difference might be due to small variations in the rate of propagation of hotspot chains, which if present would require refinements to the hotspot reconstructions. Part of the difference between these results might also be due to the possible deformation in Antarctica, which if removed from the global plate circuit would place this point further southeast (Figure 8). In any case, because the evolution of the Transantarctic rift system is still too poorly known to be included in a plate circuit, we assume that the effect is relatively small, and we ignore it.

Farallon-North America Interactions

General history of relative motions.

Menard [1978] noted that for magnetic anomalies younger than anomaly 24 the trends and spacings on the Pacific plate north and south of the Mendocino and Pioneer fracture zones were quite different, and he inferred that near the time of anomaly 24 the piece of the Farallon plate north of the Pioneer fracture zone broke off to form the Vancouver plate. Rosa and Molnar [1988] corroborated Menard's inference and determined separate parameters and uncertainties for the relative positions of the Pacific and Farallon and the Pacific and Vancouver plates after anomaly 24 time. Following Atwater and Severinghaus [1987, 1988] we assume that the trace of the Vancouver-Farallon boundary lies halfway between the Pioneer and Murray fracture zones (Figures 2f-2h).

Calculations of past positions of points on the Farallon and Vancouver plates with respect to North America (Figure 4) show that they approached from the southwest (roughly perpendicular to the present trend of the North American coast) during the interval between anomalies 30/31 and 13. The boundary between these plates and North America therefore was a subduction zone. Velocities calculated relative to fixed North America, on points adjacent to the plate boundary, reveal changes in the speed and azimuth of convergence through time (Figures 5-7). During the interval between anomalies 30/31 and 25 (68-59 Ma) the Farallon plate moved rapidly toward North America at 120 ± 50 mm/yr; the azimuth of approach varied little along the coast (Figure 5g). Between the times of anomalies 25 and 21 (56 to 50 Ma), the Vancouver plate split from the Farallon plate and the speed and azimuth of convergence varied along the coast. The velocity of the Vancouver part of the Farallon plate, relative to the North America plate, ranged from 140±50 mm/yr (in the south) to 110 ± 20 mm/yr at 45°N (Figure 6). The position of the Farallon-Kula ridge at this time is unknown, but if the Vancouver-North America boundary had extended further north and west than 45°N, the velocities there would have been even slower. For the part of the west coast of North America south of about 50°N the

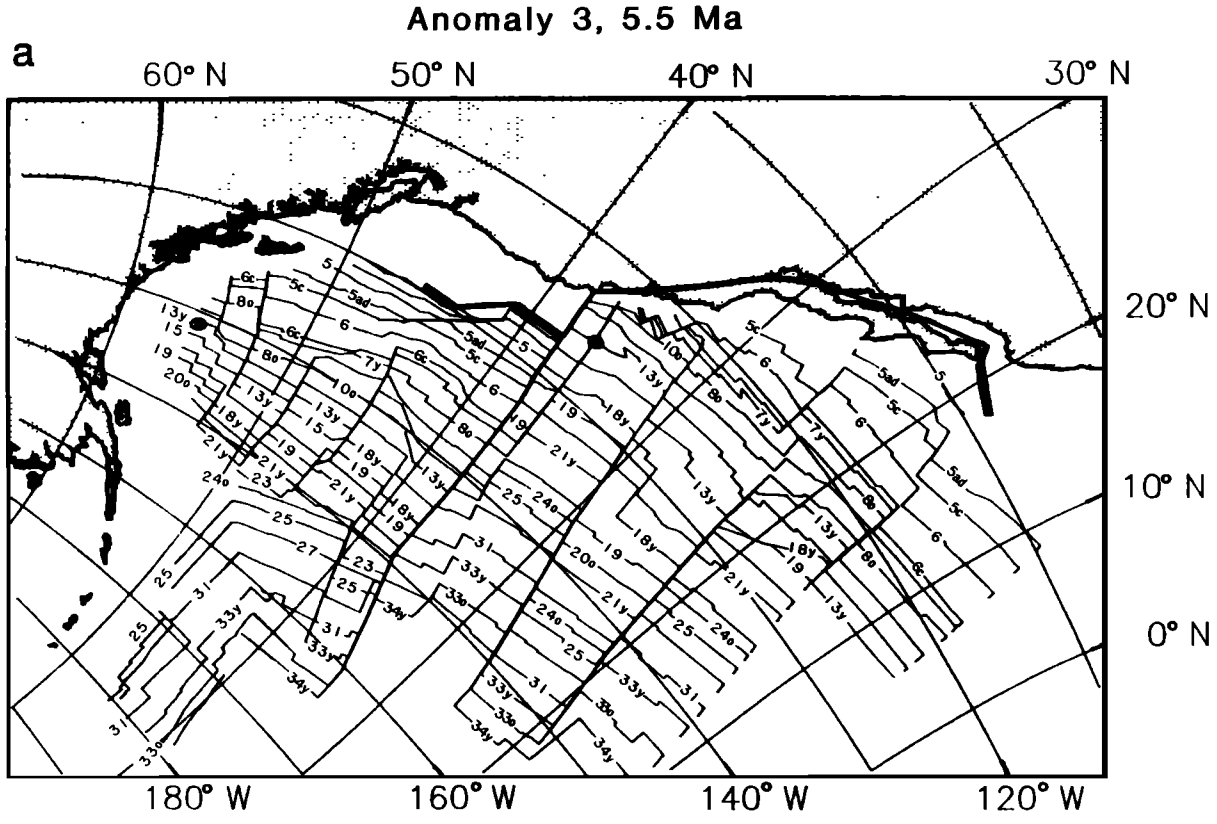

Fig. 2. Maps for 5.5 Ma and for the times of anomalies 5, 6, 7, 10, 13, 18, 21, 25, and 30/31, showing the reconstructed positions of the Pacific, Farallon, and Kula plates to North America. Symbols and map projection are the same as for Figure 1. The 1000 fm (1829 m) contour has been omitted for clarity. Continental crust west of the San Andreas fault, including the Baja California peninsula, has been reconstructed to North America using the 5.5 Ma rotation. Ellipses surrounding selected points on the Pacific plate indicate the uncertainty in the reconstructed positions of these points relative to fixed North America; uncertainties in the reconstructed positions of other Pacific plate points will be similar. The unacceptable overlap of Pacific plate oceanic crust with continental crust of North America, visible in Figures 2d-2e, may be due to extension in western North America (see Figure 8 and text). For Figures 2f-2i, rotated positions of selected magnetic isochrons (A18, A21, A25, and A30/31) on the Farallon and Vancouver plates, and their uncertainties, are also shown. Dashed heavy line in Figures 2f-2h is the approximate location of the Farallon/Vancouver boundary. For Figs. 2f-2j, plates are abbreviated as follows: K, Kula; P, Pacific; V, Vancouver; F, Farallon. Anomaly 34 is not shown on the Farallon plate because this anomaly was not studied by Rosa and Molnar [1988]; however, the distance from anomaly 34 to anomaly 30/31 on the Pacific plate may be used to estimate the position of the edge of Cretaceous Quiet Zone crust on the Farallon plate.

uncertainties are large enough that the velocity of approach could have been the same for both time intervals (A30/31 to A25 and A25 to A21).

Changes in Farallon/Vancouver-North America motion. The speeds of the Vancouver and Farallon plates relative to North America decreased during the interval between anomalies 25 and 18. Best fit velocities for the intervals between anomalies 21 and 18 and between anomalies 18 and 13 decreased (from 136 ± 47 to 85 ± 40 mm/yr in the north and from 109 ± 37 to 64 ± 24 mm/yr in the south for the two intervals, respectively; Figures 5d, 5e, and 6).

This change in plate motion (Figure 6) is more significant toward the north and

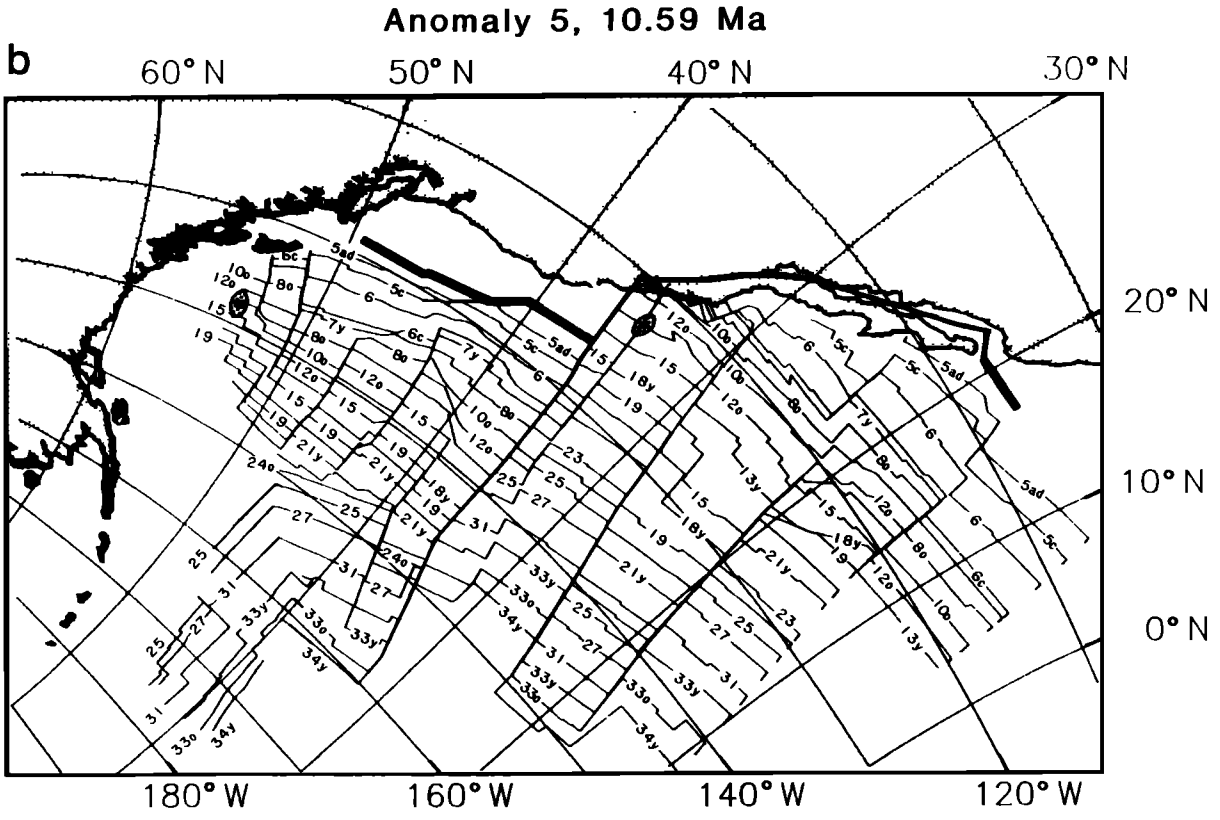

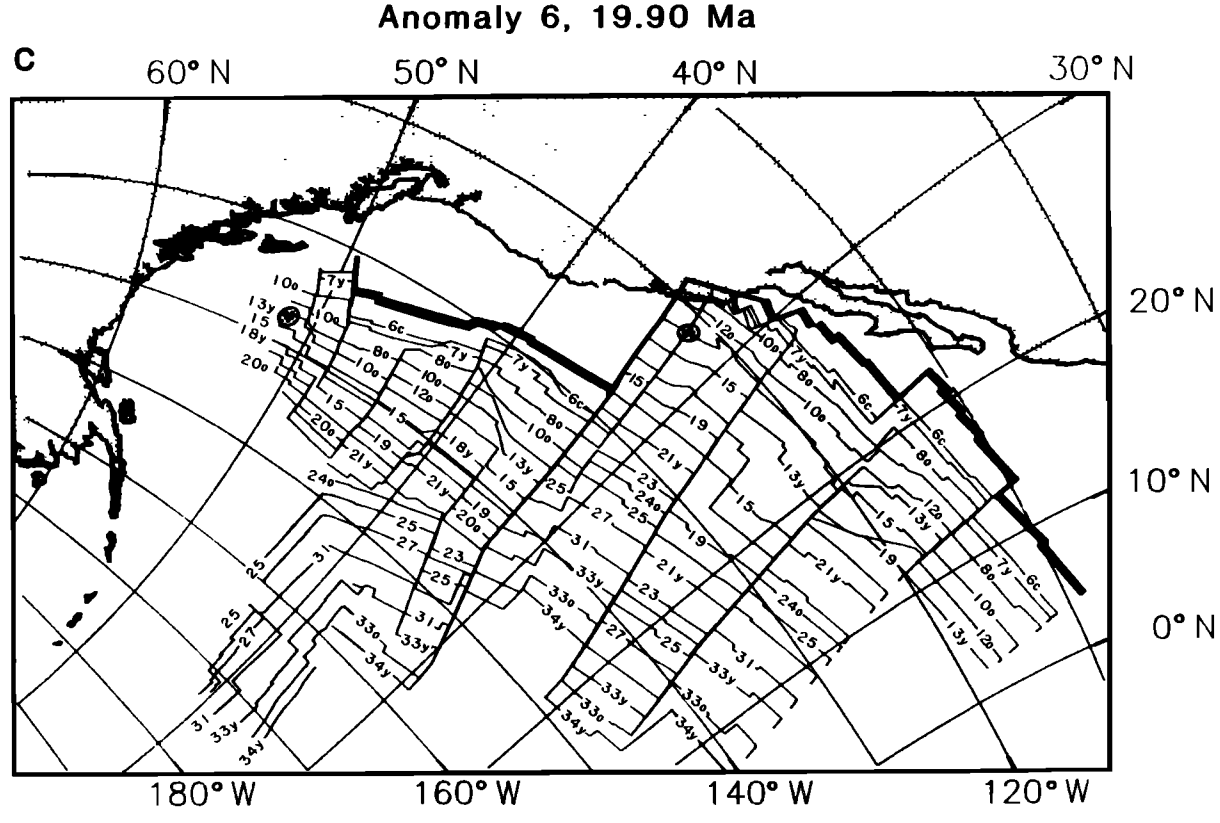

Fig. 2. (continued)

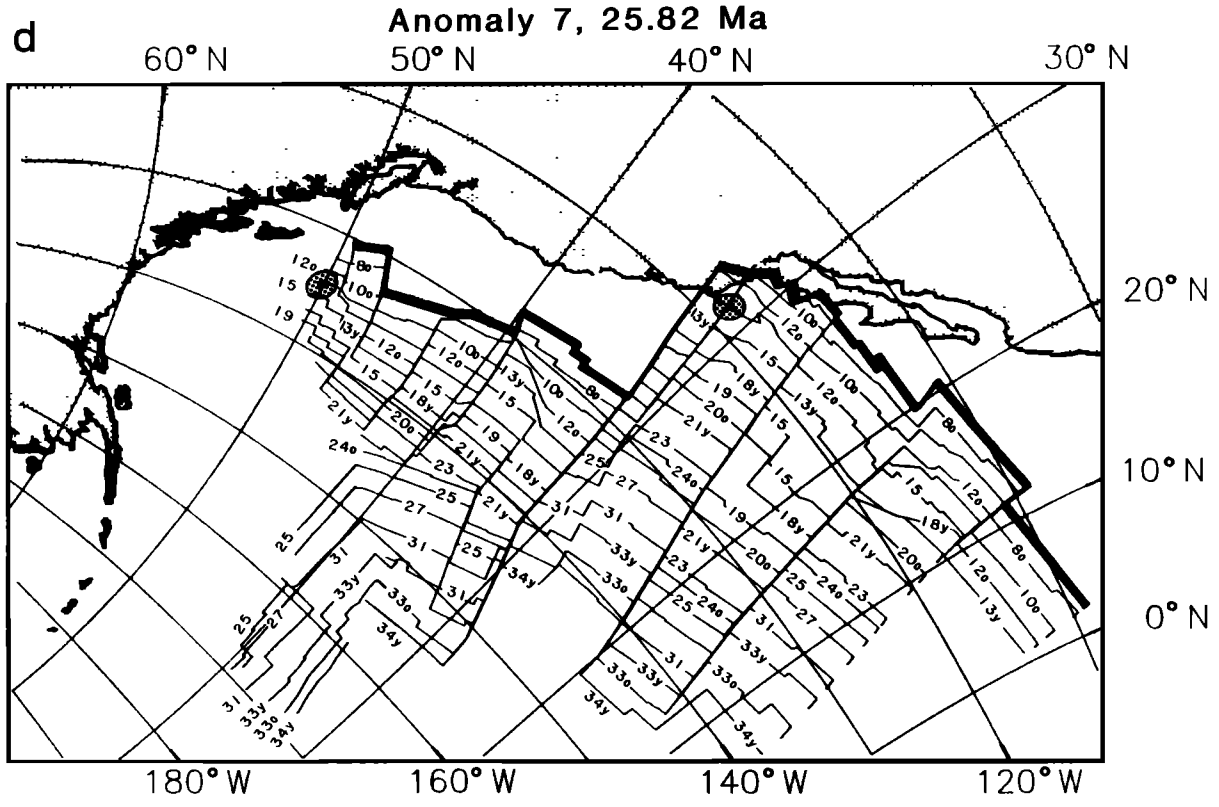

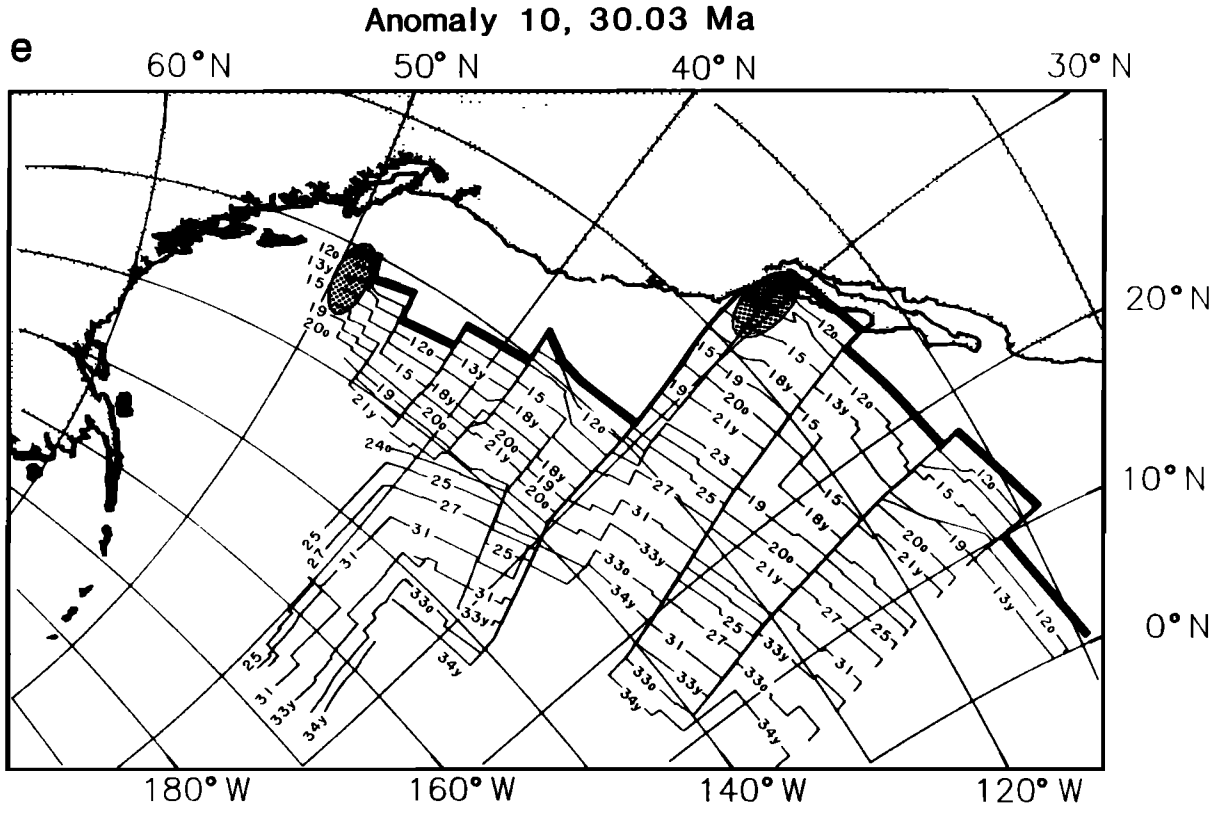

Fig. 2. (continued)

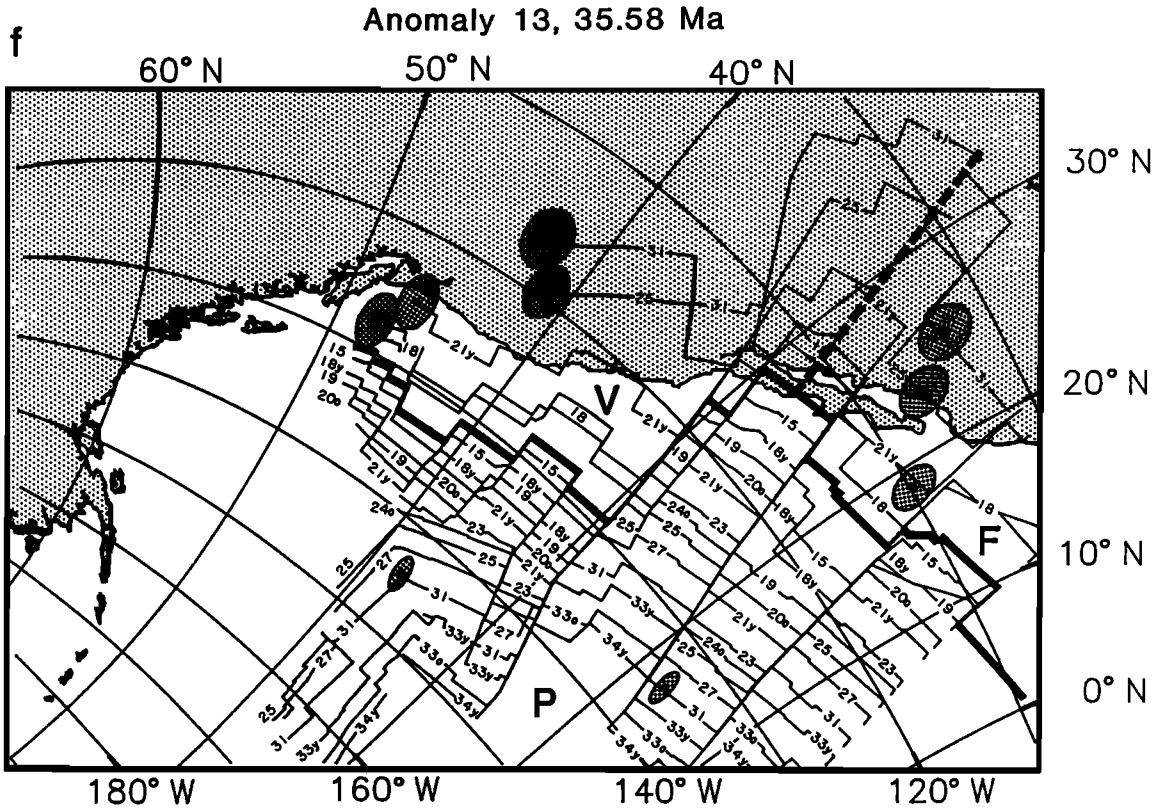

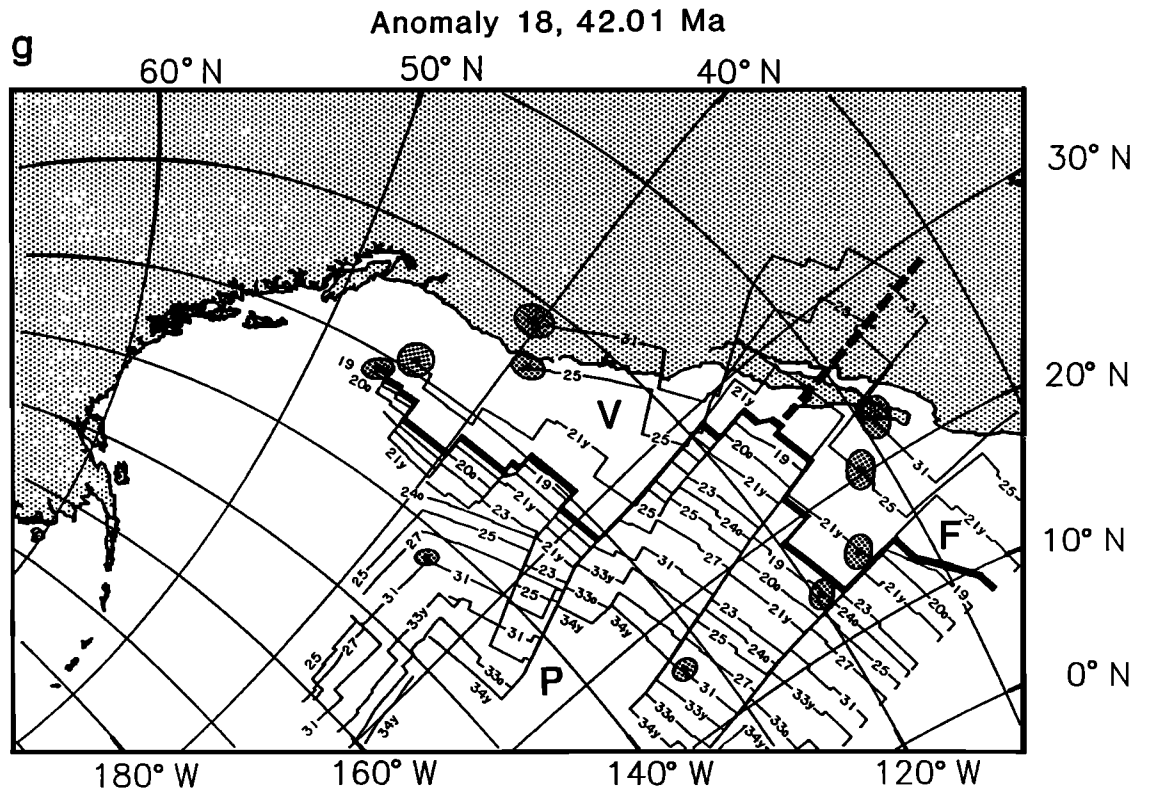

Fig. 2. (continued)

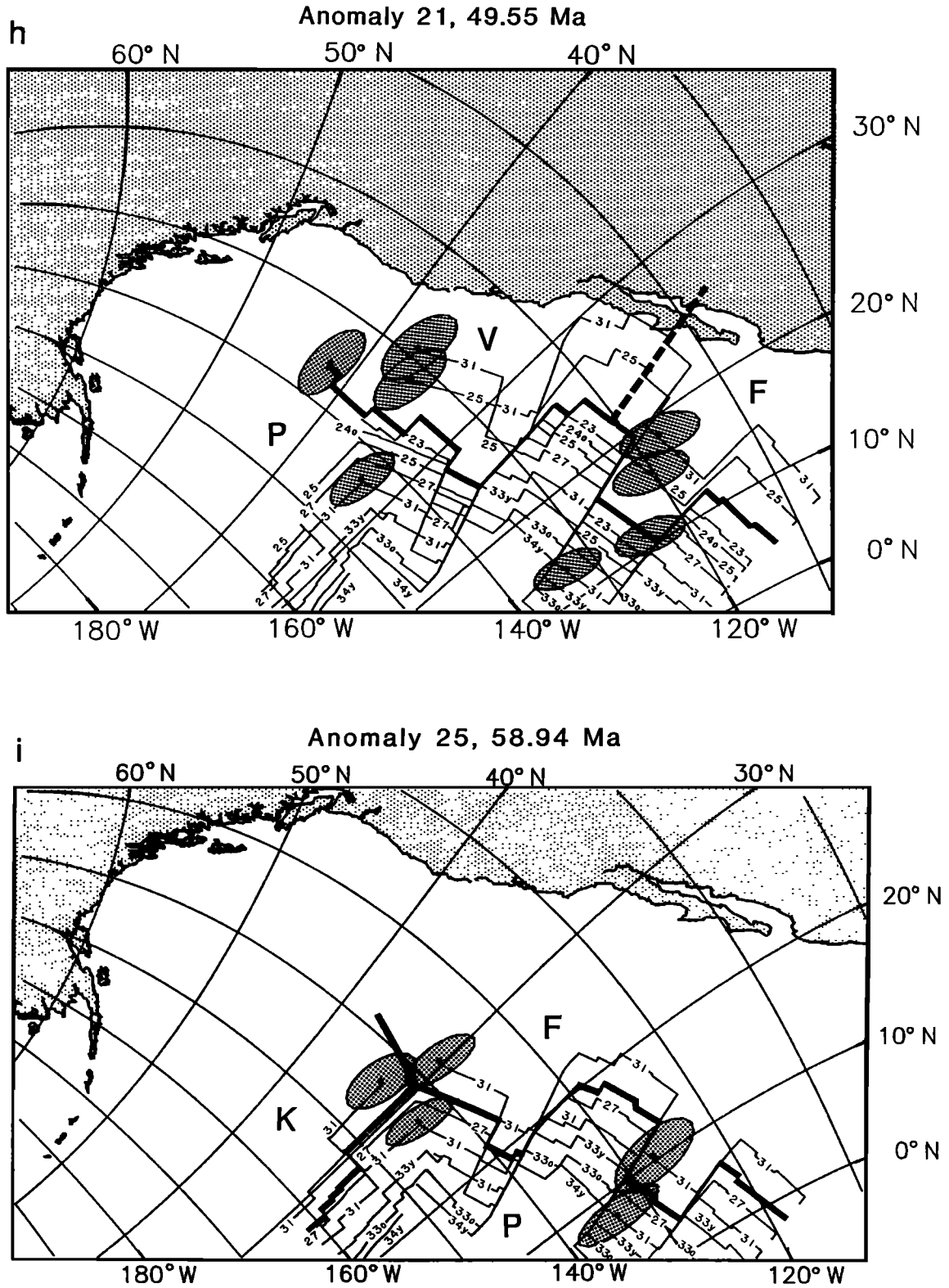

Fig. 2. (continued)

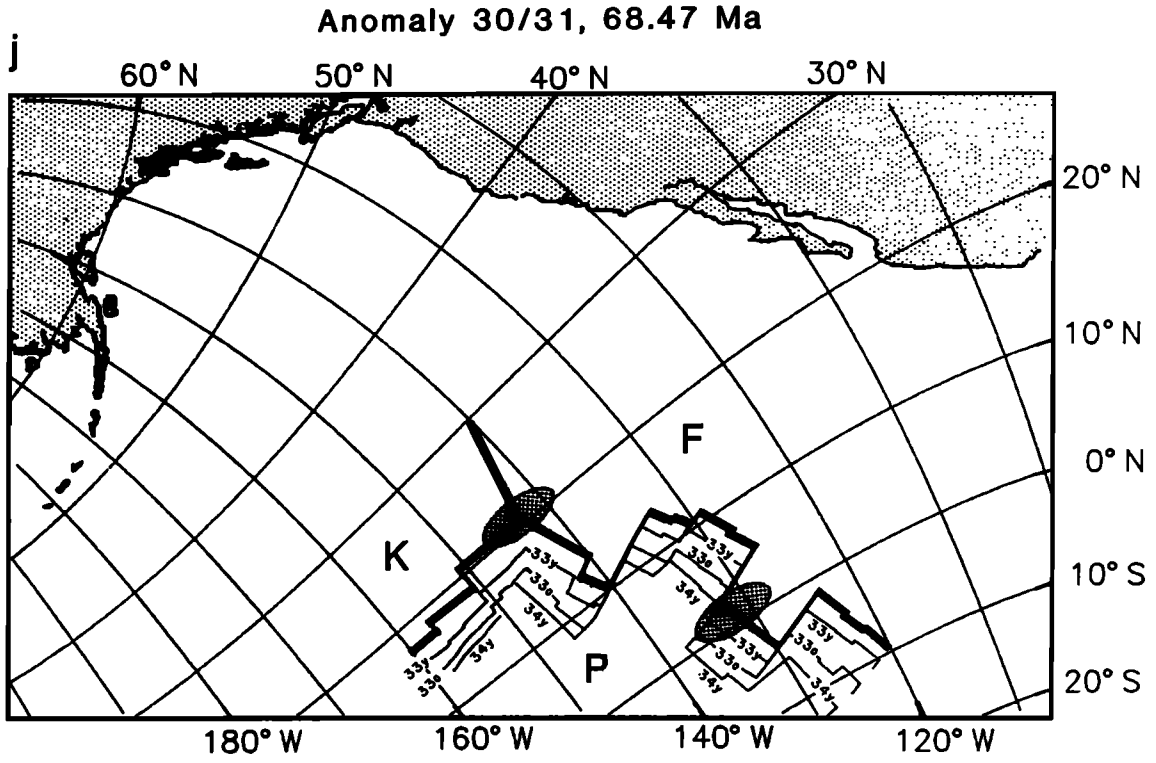

Fig. 2. (continued)

is most distinct for the two northern points studied (Figures 6d and 6e). Because the uncertainties in the velocities for the time intervals anomaly 30/31 to anomaly 25 and anomaly 21 to anomaly 18 do not overlap for latitudes north of about 45°N on fixed North America, this decrease in rate must have occurred before the time of anomaly 18 (42 Ma). The uncertainties in speed alone, or in azimuth alone, however, do overlap for these times, so that decomposition of these results into separate speeds and azimuths (Figure 7e) disguises the required difference in the velocities (Figure 6e). This decrease in convergence velocity must have occurred all along the Vancouver-North America boundary, but its magnitude decreased southward, varying from perhaps as much as a 50% decrease in speed at 45°N to no resolvable decrease at 20°N.

The time of this decrease, which probably was not abrupt, is clearly close to anomaly 21 time (50 Ma); it is definitely younger than anomaly 25 and older than anomaly 18. It is linked to two changes in motion within the plate circuit: primarily, the ~50 Ma slowdown in Pacific-North America motion, associated with the change in Africa-North America spreading direction discussed above, and secondarily, the separate motions of the Farallon and Vancouver plates after anomaly 24 time. The resultant decrease in Vancouver-North America relative velocity along the west coast of North America definitely predates the 43 Ma bend in the Hawaiian-Emperor seamount chain [Clague and Dalrymple, 1988] and the 40 Ma "end" of the Laramide orogeny [Coney, 1972]. This result differs from the conclusions drawn in some other studies based on the assumption of fixed hotspots [e.g., Coney 1978; Engebretson et al., 1984b, 1985], which reported (1) that Farallon-North America motion slowed at about 40 Ma, approximately the time of the Hawaiian-Emperor bend; and (2) that the time of this slowdown correlated with the end of the Laramide orogeny.

The previously discussed change in direction of the Pacific plate relative to North America, which occurred at about anomaly 18 time, has little effect on Farallon-North America relative motion because the divergence of the Farallon and Pacific plates before and after anomaly 18

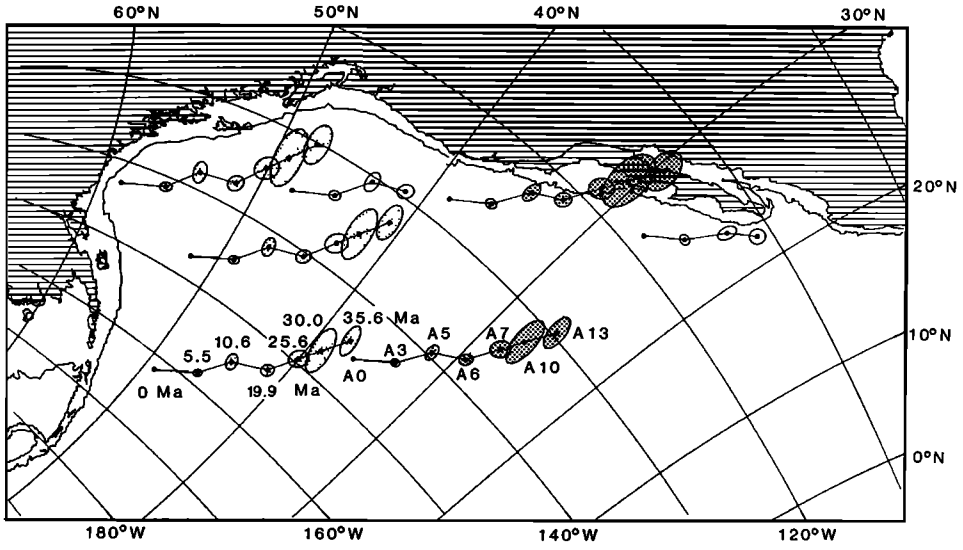

Fig. 3. Cumulative displacement of seven points on the Pacific plate, relative to fixed North America, for 0 Ma, 5.5 Ma, and the times of anomalies 5, 6, 7, 10, and 13. The times of these reconstructions (0 Ma to 35.6 Ma) are shown for the point on the lower left, corresponding to the anomalies indicated on the path of the point to the right. Ellipses indicate the uncertainties in the best fit point positions. Two of these points are on 20 Ma oceanic crust and hence their pre-20 Ma (pre-A6) positions are not shown. The linearity of the best fit motion between the times of anomalies 6 and 13 is due to the use of interpolations in the plate circuit for the times of anomalies 7 and 10. Note that the lines connecting the points are not the actual paths of motion between the two time intervals.

was much faster than Pacific-North America relative motion during these intervals.

Kula-North America Interactions

Position of the Kula-Farallon ridge with respect to North America. The orientation and position of the Kula-Farallon boundary is very poorly constrained in reconstructions for early Tertiary time [e.g., Atwater, 1970]. After 85 Ma it could have intersected the west coast of North America at any point from Vancouver to Mexico; by about 60 Ma it could have been anywhere north of about 35°N relative to fixed North America. Thus young crust of the Farallon and Kula plates, adjacent to the Kula-Farallon ridge, might have been continuously subducted beneath part of western North America in Late Cretaceous or early Tertiary time.

Cessation of Kula-Pacific spreading. Our reconstructions do not treat the Kula plate as a separate plate for times younger than anomaly 24 (55 Ma) because data regarding its motion at these times are lacking. At about the time of anomaly 24, spreading apparently stopped along the eastern end of the Pacific-Kula ridge [Byrne, 1979]. This resulted in the formation of the well known "Y-shaped" anomaly in the Gulf of Alaska and was accompanied by a change in the direction of spreading along the former Kula-Farallon boundary, with consequent reorientations of ridge crests and fracture zones and readjustments of Pacific-Vancouver spreading directions until about the time of anomaly 21 [e.g., Caress et al., 1988].

This cessation of spreading at the time of anomaly 24 may indicate complete death of this segment of the Pacific-Kula ridge or a ridge jump to another location far to the north, as suggested by Fox [1983]. If a ridge jump occurred, spreading would have continued along a more northern ridge that has now been entirely subducted. Very rapid Pacific-Kula spreading during the period from anomalies 24 to 23 (56 to 52 Ma) was proposed by Engebretson et al. [1984a] in order to explain some short, E-W trending anomalies just north of the "Y"

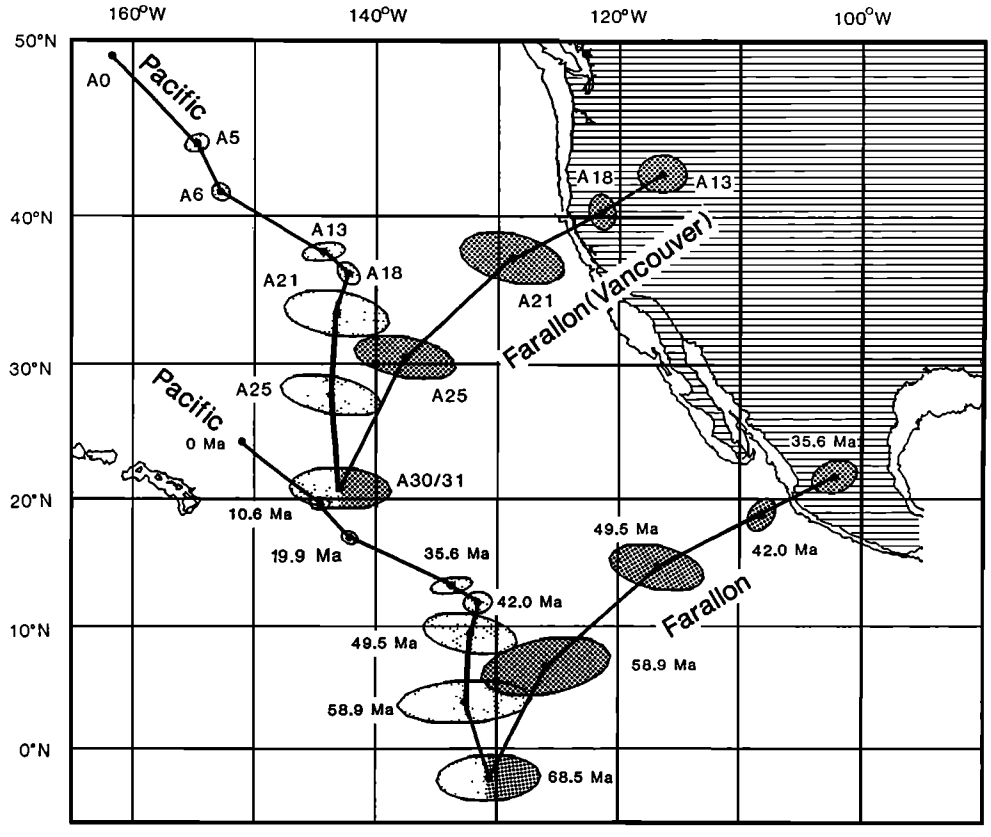

Fig. 4. Cumulative displacement of two points on the Pacific plate, relative to North America, for the times of anomalies 0, 5, 6, 13, 18, 25, and 30/31. The times (0 Ma to 68.47 Ma) are listed for the southern point and corresponding anomalies (A0 - A30/31) for the northern point. Ellipses indicate the uncertainty in the point positions. These points are both anomaly 30/31 identifications and hence would have been on the Pacific-Farallon ridge at anomaly 30/31 time. The positions and uncertainties for corresponding anomaly 30/31 age crust of the Farallon plate (southern point) and Farallon/Vancouver plate (northern point) are indicated for A30/31, A25, A18, and A13 times. Note that the lines connecting sequential positions of the points indicate net displacements but not actual paths of displacement of these points.

anomaly. Engebretson et al. [1985] assumed that this rapid spreading continued until about anomaly 18 time, although all of the relevant Kula, Farallon, and Pacific plate magnetic crust younger than anomaly 23 has been subducted. As Atwater [1988] noted, this interpretation cannot easily explain the parallelism of anomaly 20 and younger lineations north and south of the Sila fracture zone on the Pacific plate. A portion of the Pacific-Kula spreading ridge, now part of the Pacific plate near the Aleutian trench, was active until anomaly 19 time, but it rotated progressively after anomaly 24 time and spread too slowly to support Engebretson et al.'s [1985] scenario [Lonsdale, 1988]. This suggests that, even if along the entire Pacific-Kula ridge spreading continued after a ridge jump, the earlier Pacific-Kula spreading rates and directions should not be extrapolated to times younger than anomaly 24.

Kula-North America convergence velocities. Kula-Pacific reconstructions for A30/31-A25 were computed assuming symmetric spreading because an insufficient record of the relevant Kula plate magnetic anomalies remains. However, a small piece of crust of the Pacific plate south of the Aleutian trench was interpreted by Lonsdale [1988] as A30/31 age Kula plate crust added to the Pacific plate by a

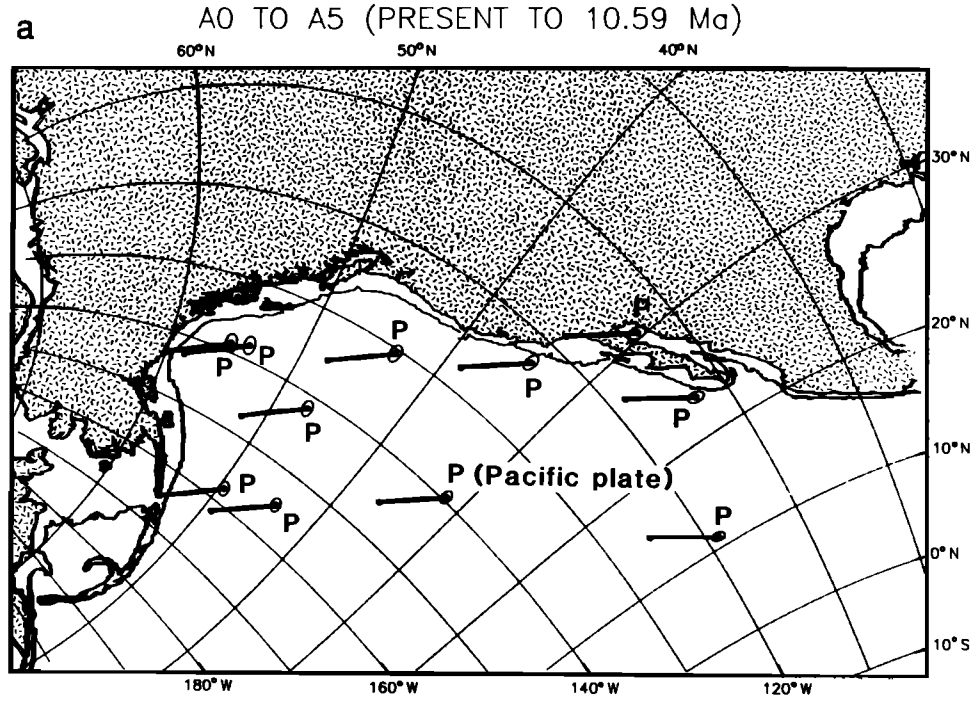

Fig. 5. Average displacements (relative to fixed North America) and the corresponding uncertainties, for points on plates adjacent to the west coast of North America, during the intervals between anomalies 0-5, 5-6, 6-13, 13-18, 18-21, 21-25, and 25-30/31. For a point at a certain position at the end of the time interval, the uncertainty ellipse surrounds its possible positions at the beginning of the time interval. Solid bar connects the best fit position of the point at the beginning of the time interval with its position at the end of the time interval, indicating the best fit displacement during the time interval. This does not necessarily indicate the path of displacement of the point. Map projection as in Figure 1. Figures 5a-5c illustrate the motion of the Pacific plate (P) relative to North America; Figures 5d-5f illustrate the Farallon (F) and/or Vancouver (V) plates, according to which plate should have been adjacent to the coast at that time. Figure 5g shows motion of both the Farallon (F) and Kula (K) plates, for each point studied, because of uncertainty regarding the position of the Farallon-Kula plate boundary during this time interval.

ridge jump. The spacing of anomalies 30 and 31 in this small region suggests that Kula-Pacific spreading during this interval was asymmetric, with more crust accreted to the Pacific plate than to the Kula plate. If asymmetric spreading also prevailed further east, the assumption of symmetric spreading overestimates the convergence rate between the Kula plate and the North America plate.

Assuming symmetric Kula-Pacific spreading between the times of anomalies 30/31 and 25 (68 to 59 Ma), the Kula plate would have been subducted at a rate of 142±30 mm/yr at an azimuth varying from 7°E ± 27°, in the east, to 19°W ± 27° at the western end of the Alaska peninsula (Figure 5g). Crust subducted under western North America could have belonged to either the Farallon or the Kula plate. The average velocity of approach of the Kula plate to fixed North America during this time interval would have decreased toward the south, to a value of 118 ± 65 mm/yr at 20°N latitude, but its azimuth of approach would have been N10°E ± 27°, with very little latitudinal variation. This corresponds to a component of strike-slip motion, parallel to the present coastline, ranging from 59 ± 32 mm/yr at 20°N to 113 ± 29 mm/yr at 45°N.

The uncertainties in these velocities include the velocities given by Engebretson et al. [1985] for times prior

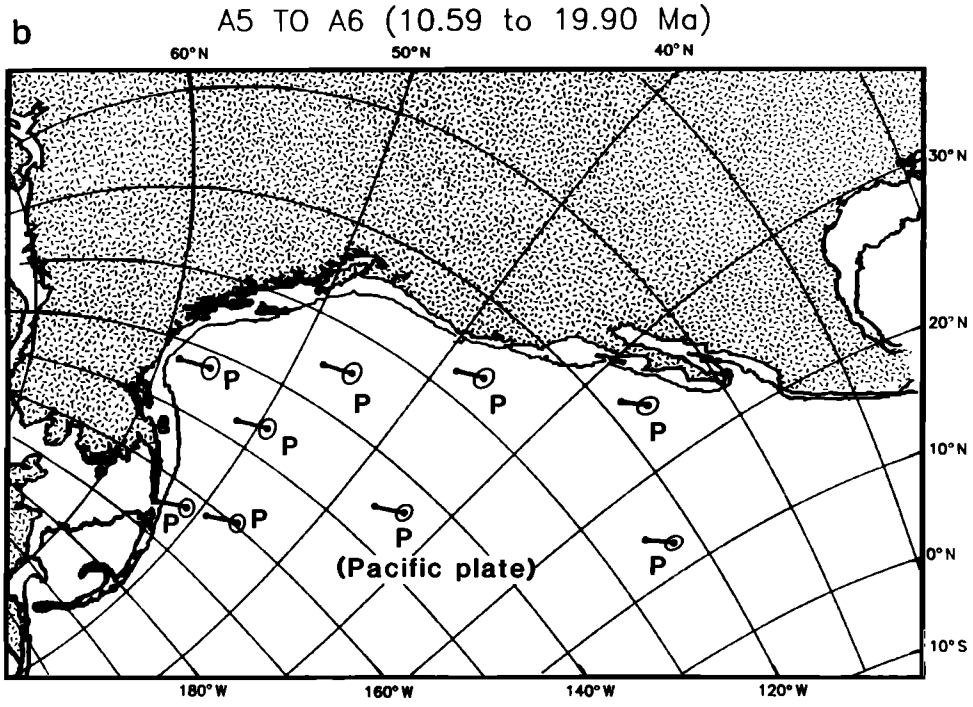

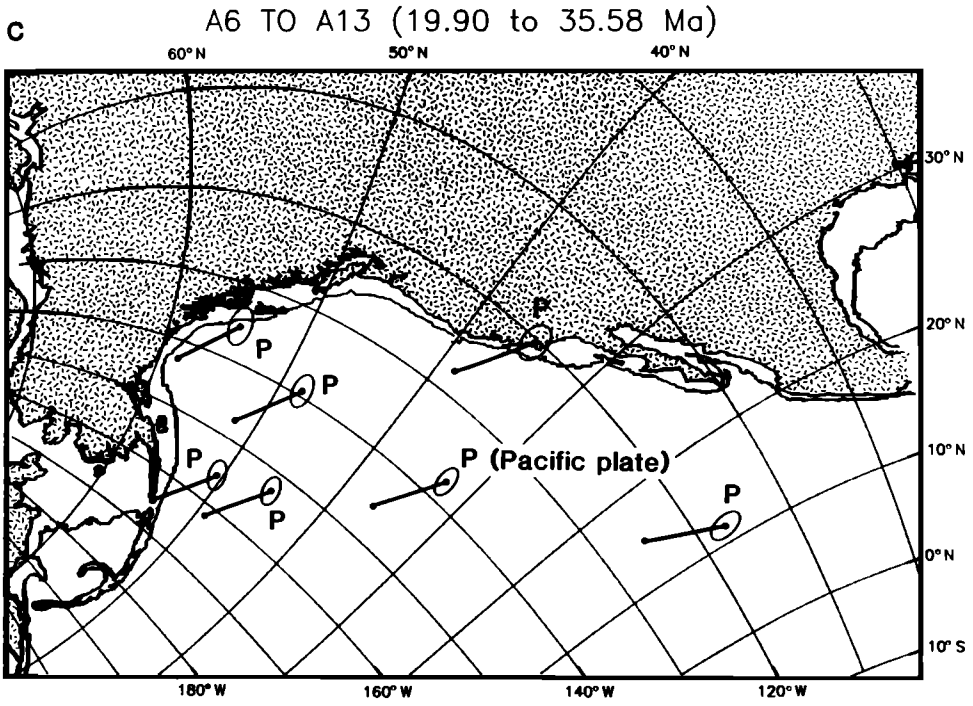

Fig. 5. (continued)

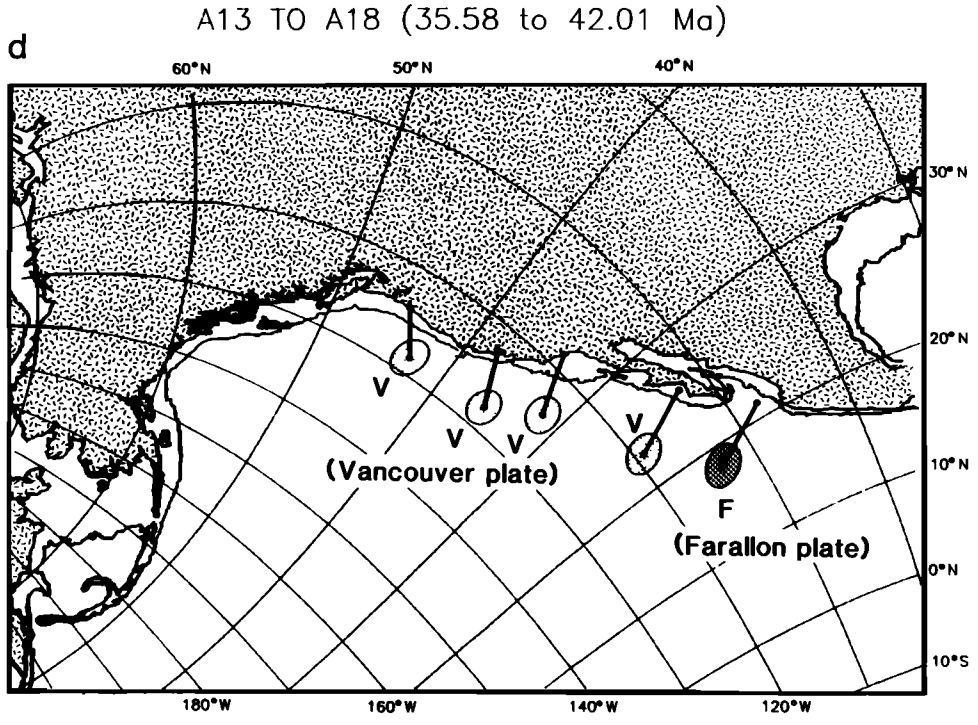

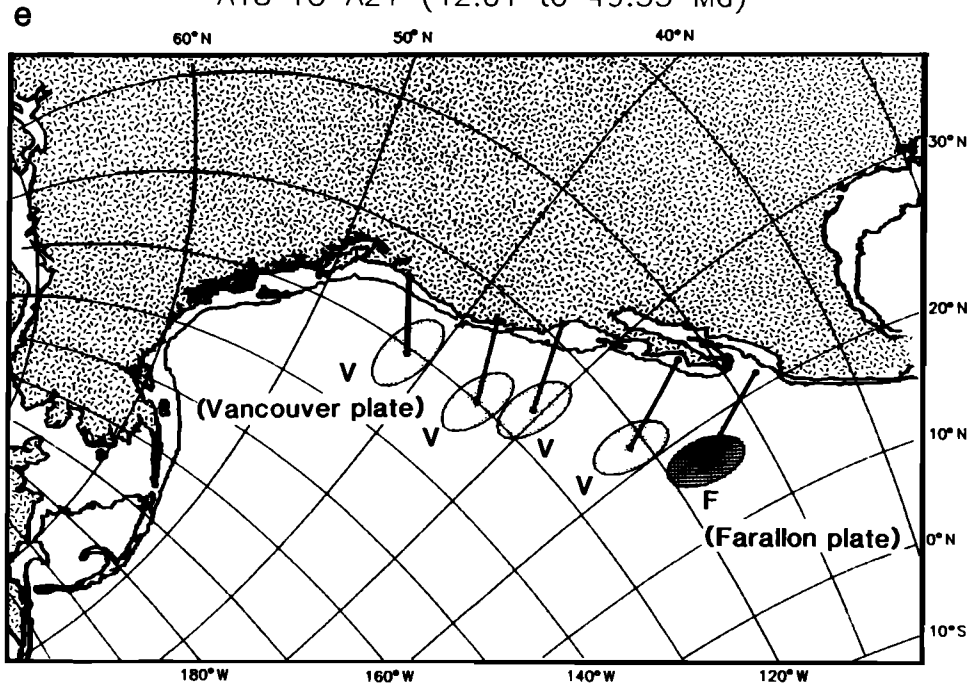

Fig. 5. (continued)

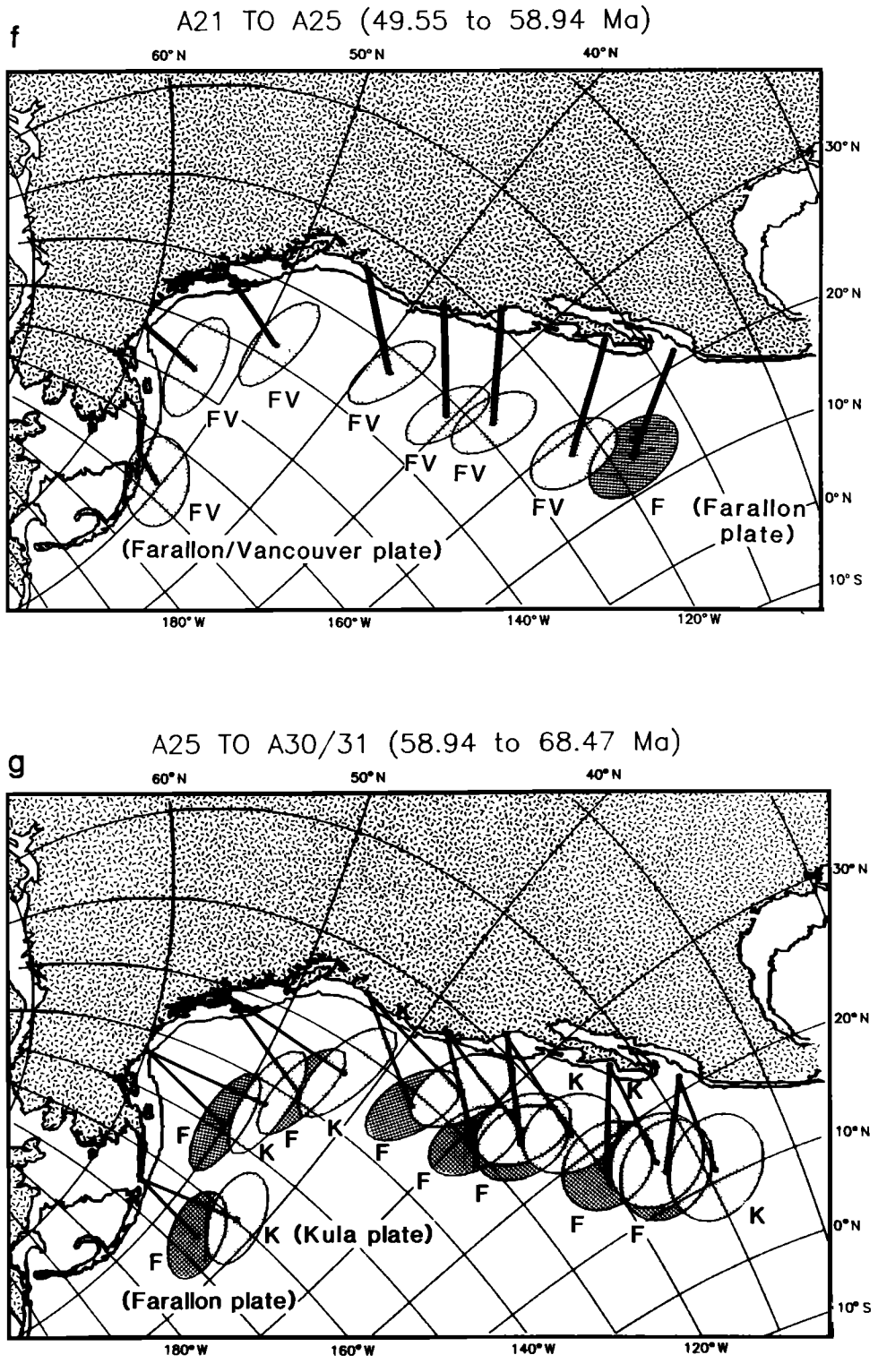

Fig. 5. (continued)

TABLE 15. Approach of the Pacific, Farallon, and Vancouver Plates to North America

Point	Anomaly Interval	Distance, km	Azimuth	Time Interval, m.y.	Speed, mm/yr
Northern Point on Pacific plate	A31-A25	770 ± 380	N6°W ± 55°	9.53	81 ± 40
	A25-A21	610 ± 260	N4°E ± 52°	9.39	65 ± 28
	A21-A18	320 ± 260	N16°E ± 60°	7.54	42 ± 34
	A18-A13	240 ± 195	N49°W ± 52°	6.43	37 ± 30
	A13-A6	830 ± 160	N59°W ± 12°	15.68	53 ± 10
	A6-A5	335 ± 55	N24°W ± 26°	9.31	36 ± 6
	A5-0 Ma	740 ± 70	N48°W ± 6°	10.59	70 ± 7
Southern Point on Pacific plate	A31-A25	735 ± 330	N16°W ± 70°	9.53	77 ± 35
	A25-A21	625 ± 220	N5°E ± 62°	9.39	67 ± 23
	A21-A18	310 ± 290	N15°W ± 70°	7.54	41 ± 38
	A18-A13	270 ± 230	N55°W ± 55°	6.43	42 ± 36
	A13-A6	950 ± 110	N64°W ± 12°	15.68	61 ± 7
	A6-A5	360 ± 140	N37°W ± 21°	9.31	39 ± 15
	A5-0 Ma	810 ± 60	N47°W ± 5°	10.59	76 ± 6
Vancouver plate	A31-A25	1200 ± 370	N25°E ± 35°	9.53	126 ± 39
	A25-A21	1100 ± 450	N38°E ± 35°	9.39	117 ± 48
	A21-A18	750 ± 300	N60°E ± 30°	7.54	99 ± 53
	A18-A13	500 ± 240	N60°E ± 30°	6.43	78 ± 37
Farallon plate	A31-A25	1170 ± 570	N28°E ± 44°	9.53	123 ± 60
	A25-A21	1360 ± 680	N48°E ± 34°	9.39	145 ± 72
	A21-A18	1000 ± 560	N63°E ± 25°	7.54	133 ± 74
	A18-A13	680 ± 360	N63°E ± 22°	6.43	106 ± 56

to Anomaly 25 but not for subsequent times. For the period 56-43 Ma, Engebretson et al. [1984b, 1985] reported velocities exceeding 200 mm/yr for Kula-North America convergence at the Aleutian arc because of their assumption of more rapid Kula-Pacific spreading throughout this interval than occurred prior to anomaly 24 [Engebretson et al., 1984a]. As discussed above, there is more evidence to favor the interpretation that Kula-Pacific motion had either slowed or ceased early in this interval.

These different sets of assumptions imply very different amounts of early Tertiary northward motion of the Kula

TABLE 16. Total Displacement Between the Pacific and North America Plates Since 30 Ma

Anomaly Interval	Distance, deg	Distance, km	Azimuth East of North	Time Interval, m.y.	Speed, mm/yr
0-3	2.92 ± 0.4	325 ± 45	-34 ± 6	5.5	59 ± 3
0-5	5.68 ± 0.6	635 ± 70	-47 ± 6	10.59	60 ± 7
0-6	7.85 ± 0.6	875 ± 70	-49 ± 3	19.90	44 ± 4
0-7	10.41 ± 0.9	1160 ± 100	-49 ± 4	25.82	45 ± 4
0-10	12.20 ± 0.8	1360 ± 90	-52 ± 9	30.03	45 ± 3

Displacements calculated for a Pacific plate point now near the Mendocino Triple Junction.

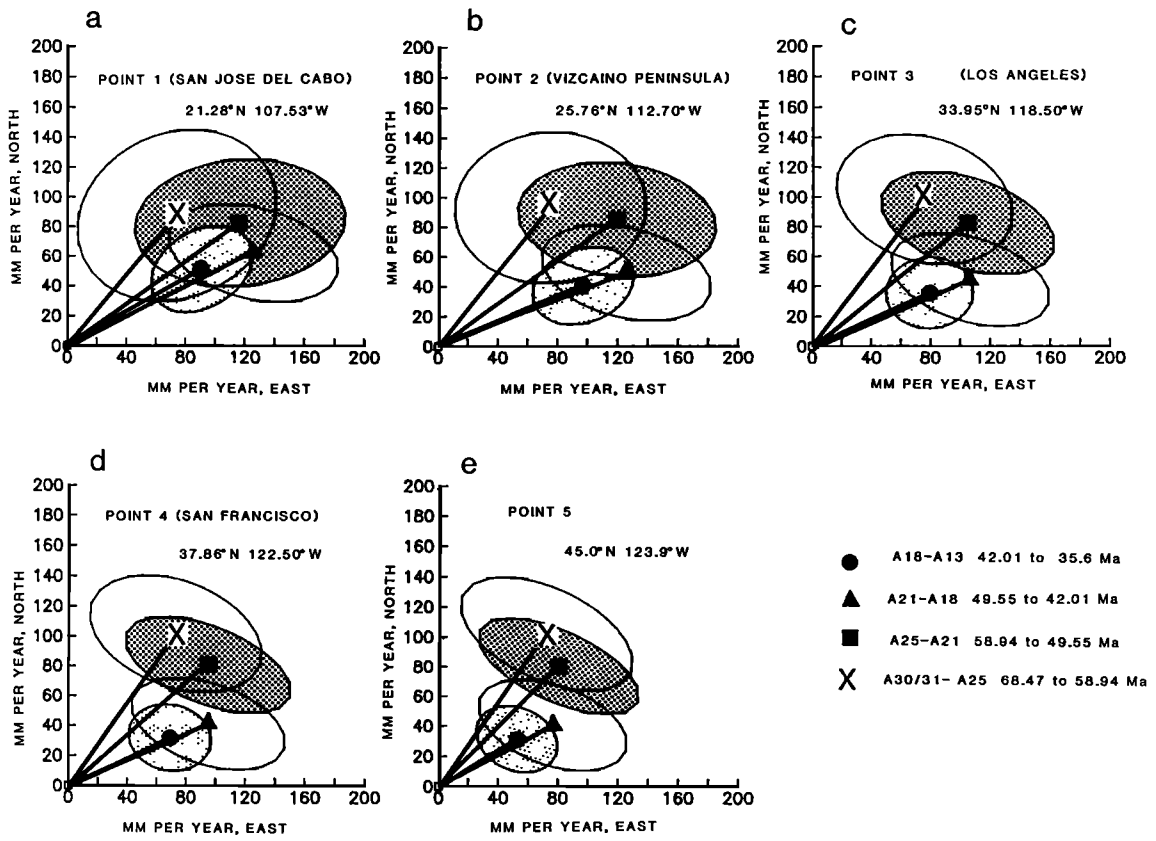

Fig. 6. Average convergence velocity between the Farallon/Vancouver and North America plates at five points on the west coast of North America (southern five of the points shown in Figure 5). Ellipses represent the uncertainty in the velocity vector. Note that at point 5 (Figure 6e), the average velocities during the intervals A30/31-A25 (cross) and A21-A18 (triangle) could not have been the same. Uncertainty ellipses for the time intervals A25 to A21 and A18 to A13 are shaded for clarity.

plate relative to fixed North America. If Pacific-Kula spreading ceased at anomaly 24 time, points on the Kula plate would have moved northward 2500 ± 400 km between anomaly 30/31 and anomaly 18 time. This is much less than the ~4300 km of northward motion expected under Engebretson et al.'s [1984a] assumptions. Clearly a longer duration of Kula-Pacific spreading, at a very fast rate, is more favorable for explaining rapid northward transport of allochthonous crustal blocks during early Tertiary time; unfortunately, the critical seafloor evidence regarding spreading rates during this interval is lacking.

Plate Tectonics and the Laramide Orogeny

Traditionally, the phrase "Laramide orogeny" refers to Late Cretaceous to Eocene compressional deformation in or east of the Cretaceous cordilleran thrust front in western North America [Armstrong, 1968, 1974]. Global plate reconstructions indicate that during most of this period the Farallon and Vancouver plates were being subducted eastward under North America, and the Kula plate was being subducted toward the northeast or north. The obliquity of subduction varied with the orientation of the coastline but changed abruptly where the Kula-Farallon ridge intersected the coast (Figure 5g). As discussed above, by the end of the Laramide orogeny the Kula plate was probably moving as part of the Pacific plate. In considering possible links between plate motions and geologic deformation during this time interval the style and lateral extent of geologic

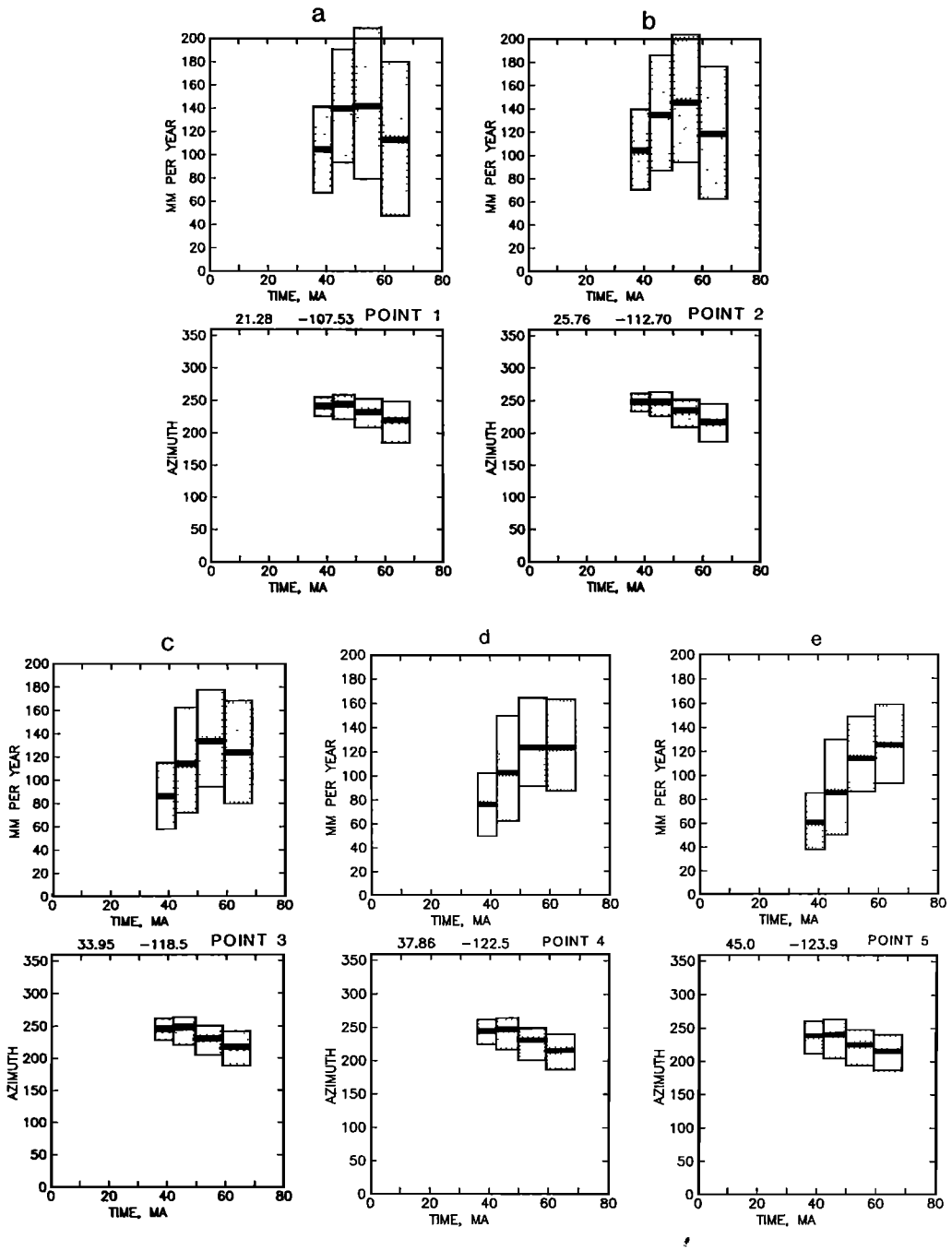

Figure 7. Speed and azimuth of convergence through time, for the same points as in Figure 6, on the west coast of North America. Uncertainty bars are derived from the uncertainties in Figure 6. Note that the uncertainties in speed and azimuth for the intervals A30/31-A25 and A21-A18 overlap for point 5 (Figure 7e), although the velocities are mutually exclusive (Figure 6e).

structures, the timing of deformation, and the history of volcanism must each be examined.

Structural style. From Late Cretaceous through Eocene time, crustal shortening from Montana and Wyoming south to New Mexico was accommodated primarily on thrust and reverse faults that penetrated

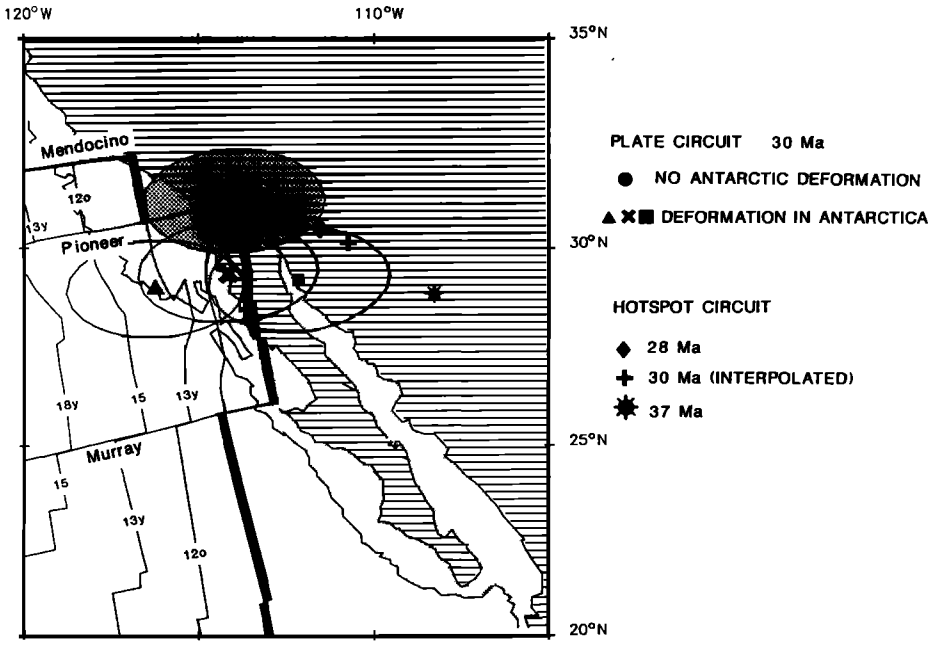

Figure 8. Reconstruction of the Pacific plate to fixed North America at the time of anomaly 10 (30.03 Ma). Reconstruction and isochrons as in Figure 2e. Crust shallower than the 1000 fm (1829 m) bathymetric contour is shaded. Continental crust west of the present San Andreas fault/Gulf of California has been restored to North America by the 5.5 Ma reconstruction. Black dot is on the anomaly 10 ridge immediately south of the Pioneer fracture zone. The shaded ellipse indicates the uncertainty in position of this point, corresponding to an overlap of 340±200 km between the northern end of this ridge segment and continental crust. Other symbols in ellipses show the positions of the same point if 200 km of post-30 Ma extension were removed from the Transantarctic rift system by moving West Antarctica relative to East Antarctica by one of three representative rotations: square, 45°S, 150°E, -3.0°; cross, 0°S, 150°E, -1.8°; triangle, 45°S, 30°W, 3.0°. Diamond, plus sign, and star are the positions of the same point relative to North America after rotation by the 28 Ma, 30 Ma, and 37 Ma fixed hotspot reconstructions of Engebretson et al. [1985]. Note that the fixed hotspot reconstructions indicate even more overlap than the global plate circuit reconstructions. See text for discussion.

into the basement, east of the previous Sevier thin-skinned thrust belt. North and south of this zone, crustal shortening along low-angle thrust faults persisted well into Paleocene time [Armstrong, 1974]. This along-strike variation in structural style and associated geochemical and spatial patterns of magmatism have been attributed to variations in dip of segments of the subducted Farallon plate [e.g., Burchfiel and Davis, 1975; Coney and Reynolds, 1977; Cross and Pilger, 1978, Dickinson and Snyder, 1978; Lipman et al., 1971].

In the present Andean orogenic belt there are analogous variations in the distance from the trench to the edge of the deformational belt, the style of compressional structures, and the arc-trench distance. These variations correlate with alternating steeply and shallowly dipping segments of the Nazca plate presently being subducted beneath South America [Jordan et al., 1983], but no cause and effect relationship between the tectonics of the upper plate and the dip of the slab is clear. The boundaries between segments of constant dip of the Nazca plate do not correlate in a simple fashion with variations in the age of the crust being subducted nor with along-strike variations in Nazca-South America convergence rate [Pilger, 1981, 1984]. Variations in the tectonic style of the

upper plate and the segmentation of the downgoing slab may both be controlled by preexisting structures either in the downgoing plate [e.g., Pilger, 1981] or the overriding plate, as well as by the shape of the subduction zone [Jordan et al., 1983]. Even if all of these variables were known for the former Farallon (Vancouver)-North America subduction zone, the past positions of fracture zones, spreading ridges, and oceanic plateaus on the subducted plate, relative to the fixed upper plate, cannot yet be reconstructed accurately enough to test detailed correlations for the Laramide orogeny.

Elsewhere in the world, Laramide-type basement deformation has occurred without a shallowly dipping slab beneath it. For instance, the active mountain range that seems most analogous to the Colorado-Wyoming Rockies, where basement uplift along thrust and reverse faults was the mode of crustal shortening, is the Tien Shan in Asia, beneath which no oceanic lithosphere has been subducted since the Paleozoic era [Molnar and Lyon-Caen, 1988; Nelson et al., 1987]. Thus the along-strike variation of structural styles during Laramide time, including the prevalence of reverse faults in the basement, may have had causes other than segmentation and variation in dip of a subducted slab. Geochemical evidence from Upper Cretaceous and lower Tertiary volcanics in the western United States is consistent with the presence of a shallowly dipping slab, but since these volcanics are largely outside of the region of the Laramide basement uplifts, they cannot constrain the dip of the slab beneath the region most affected by high-angle basement-involved faulting.

A more general characteristic of the Laramide orogeny is that a zone of crustal shortening, rather than a narrow island arc or an interarc basin, developed inland of the subduction zone. This zone of compression extended from Canada to Mexico, encompassing both the area of the basement uplifts and the thin-skinned thrust belts to the north and south. Above presently active subduction zones, broad belts of compression tend to occur where young (<50 Ma) oceanic crust is being subducted [Molnar and Atwater, 1978]; the details of the transition from extensional to compressional upper plate tectonics depend on the age of the subducted crust, the convergence velocity, and the slab dip [England and Wortel, 1980]. Plate reconstructions can address the first two of these factors.

The reconstructed positions of the Vancouver/Farallon plate can be used to estimate the variations in ages of the subducted plate along the trench. These ages depend on both the assumed position of the trench with respect to fixed North America and the assumption of symmetric spreading. Let us ignore subsequent displacement of the continental margin due to deformation in western North America. If the trench lay at the margin, then at 40°N latitude (relative to fixed North America) the Vancouver plate entering the trench at anomaly 13 time (36 Ma) would have carried anomaly 21 (50 Ma), formed between the Sila and Sedna fracture zones, and the sea floor would have been about 14 million years old. The uncertainty of ±170 km in the position of the Vancouver plate perpendicular to the trench corresponds to an uncertainty of ±5 m.y. in the age of the crust entering the trench there. Similar reasoning for the time of anomaly 18 (42 Ma), for the trench at 40°N relative to fixed North America, yields uncertainties of ±90 km for 59 Ma crust entering the trench, corresponding to an age of subducted crust, formed just south of the Sila fracture zone on the Farallon plate, of 17 ± 4 million years.

Reconstructions of this sort for the time of anomaly 21 (50 Ma) and earlier are very poorly constrained for two reasons. First, neither the shape of the Kula-Farallon plate boundary nor the position of its intersection with the west coast of North America is well known, so that the subducted plate at the trench along much of the west coast of North America may have been either the Kula or the Farallon plate. It is difficult to express these two very different possibilities in terms of a single numerical uncertainty. Second, even if we knew that the Farallon plate were being consumed at the trench at 40°N, the crust involved would have been formed by Pacific-Farallon spreading during the Cretaceous magnetic quiet period. Even ignoring the virtually certain ridge jumps along some segments of this boundary, the age of the seafloor on the Farallon plate is very uncertain.

At the time of anomaly 25 (59 Ma), if Farallon plate crust formed at the Pacific-Farallon spreading center were being subducted, large parts of the subducting plate would have been older than anomaly 34 (84 Ma), the old edge of Pacific plate crust of well-constrained

age formed at the Pacific-Farallon ridge. The next oldest identifiable magnetic anomaly created at this spreading center is anomaly M0 (118 Ma) [Hilde et al., 1976], on the opposite side of a 1000-km-wide strip of Pacific plate oceanic crust generated during the Cretaceous magnetic quiet period. The M0 anomalies are separated from the anomaly 34 age oceanic crust by a fracture zone, and the orientation of both the magnetic anomaly lineations and the fracture zones near M0 are quite different from those near anomaly 34, suggesting that a change in direction, if not also rate, occurred during the Cretaceous magnetic quiet period [e.g., Atwater, 1988; Engebretson et al., 1984a].

Assuming symmetric Pacific-Farallon spreading between anomalies M0 and 34, we find that at the time of anomaly 25 the M0 age crust on the Farallon plate side of the Pacific-Farallon spreading center would have been close to the trench, so that the age of the crust being subducted at 40°N would have been about 60 m.y. The Farallon plate crust formed at the Farallon-Pacific ridge during the Cretaceous magnetic quiet period would have been subducted at this latitude until after the time of anomaly 21 (50 Ma), as part of the smooth decrease in age of the crust entering the trench west of North America that continues to the present [e.g., Engebretson et al., 1984b]. As noted by Engebretson et al. [1985], this result would not support a correlation between the existence of a wide zone of Laramide deformation and the subduction of young (<50 m.y. old) oceanic crust [e.g., Molnar and Atwater, 1978].

Jumps of the Pacific-Farallon ridge between the times of anomalies M0 and 34 time could have caused sharp discontinuities in the age of the crust entering the trench. Differences in age offsets of the crust along the Mendocino fracture zone at M0 time and anomaly 33 time require at least a small ridge jump to have occurred there during the Cretaceous magnetic quiet period [Engebretson et al., 1984a; Hayes and Pitman, 1970; Woods and Davies, 1982], but its magnitude, direction, and location are unknown. This is another aspect of the problem that cannot be quantified in terms of a simple numerical uncertainty.

Mammerickx and Sharman [1988] describe evidence for a large Pacific-Farallon ridge jump at about 87 Ma, which would have taken most of the Farallon plate crust formed during the Cretaceous normal period, between the Chinook trough and the Mendocino fracture zone, and transferred it to the Pacific plate. (Rea and Dixon [1983] proposed that such a transfer was not instantaneous but rather took place via the formation of a short-lived plate, the Chinook plate.) In this case, much less distance would separate crust of M0 and anomaly 34 age on the Farallon plate side of the Pacific-Farallon spreading center, and there would have been a sudden decrease in age of subducted crust, of about 30 m.y., as the position of this ridge jump (recorded on the Farallon plate) entered the trench. Although the total age change across this discontinuity is not well constrained, it would have entered the trench a few million years after anomaly 21 time (50 Ma), resulting in a change in age of the crust entering the subduction zone from 60 m.y. to 30 m.y. In this case, much of the Farallon plate crust subducted between 75 and 55 Ma would probably have been even older than 60 m.y., making it even more difficult to support a correlation between Laramide deformation and the subduction of young oceanic crust.

On the other hand, as stressed by Beck [1984] and Atwater [1988], the position and orientation of the Kula-Farallon ridge are poorly constrained by plate reconstructions. It is possible that some of the ocean floor subducted beneath western North America during Laramide time was formed at the Farallon-Kula ridge and hence was less than 50 m.y. old when it entered the trench. Thus we cannot eliminate the possibility that some of the deformation in western North America during Laramide time was due to rapid subduction of young oceanic lithosphere.

Finally, we cannot rule out the possibility that a relatively more buoyant feature such as an oceanic plateau [Henderson et al, 1984; Livaccari et al., 1981] arrived at the subduction zone anywhere north of Mexico during latest Cretaceous to Eocene time and caused the broad zone of continental deformation in the western United States during Late Cretaceous and early Tertiary time or the variation along strike of structures within this zone.

Timing of deformation. Previous workers have reported correlations between the timing of Laramide deformation (and especially of its termination), and the timing of changes in Farallon-North America plate motion [e.g., Coney, 1978; Jurdy, 1984; Engebretson et al., 1985]. Analogous correlations have been reported

for the Andes, where higher rates of subduction appear to correlate with periods of more intense tectonic activity [Pardo-Casas and Molnar, 1987]. In view of the differences between our reconstructions and previous reconstructions of Farallon-North America motion we reexamine some of these correlations below.

Early Laramide deformation began in Campanian time (83-73 Ma) and may have been transitional from yet earlier deformation related to the Sevier orogeny. We cannot constrain the rates of Farallon-North America motion during this period because it entirely predates our earliest reconstruction. In many areas, deformation ended by the end of Paleocene time (55 Ma) [e.g., Armstrong, 1974], but intense and possibly separate phases of faulting continued in certain areas through early or mid-Eocene time [Tweto, 1975]. A 40 Ma age for the end of the Laramide orogeny [Coney, 1972] has often been assumed. However, within the central Rocky Mountain region, existing data suggest that Laramide deformation ended diachronously, as early as 55 Ma in the north and as late as 35 Ma to the south [Dickinson et al., 1988]. The relative amount of Laramide crustal shortening through time may be an alternative way to identify the "end" of the Laramide orogeny but is not well constrained.

A 40-35 Ma time of cessation of Laramide deformation, and in particular a progressive cessation, does not obviously correlate with the roughly 56-50 Ma decrease in Farallon(Vancouver)-North America convergence rate. This may be because either (1) the end of the Laramide orogeny was dominantly controlled by factors unrelated to convergence rate [e.g., Dickinson et al., 1988]; (2) the end of the Laramide orogeny was controlled by changes in the thermal structure of the subducted slab, which were delayed responses to changes in the convergence rate [Severinghaus and Atwater, 1987 and manuscript in preparation, 1988]; or (3) the end of the Laramide orogeny was directly related to changes in convergence rate, but these changes were more dramatic to the north than to the south and hence affected the crustal tectonics earlier to the north. Until the timing of cessation of the Laramide orogeny is better constrained throughout its extent, any of these hypotheses (or a combination of them) appear to be viable.

The early to mid-Eocene phase of Laramide deformation, in which E-W trending structures were most active, has been interpreted as a progressive counterclockwise rotation of the orientation of crustal shortening through time, from ENE to a more northerly trend, in the region of the basement uplifts [Gries, 1983; Chapin and Cather, 1983]. Our reconstructions suggest that the convergence vector between the Farallon and North America plates would have rotated in the opposite sense (clockwise) during this time. The orientations of the Laramide basement uplifts have also been attributed to the counterclockwise rotation of the Colorado Plateau relative to the craton [Hamilton, 1978]. This would result in spatial variation, rather than temporal variation, of the compression direction. No major latitudinal variation in Farallon(Vancouver)-North America convergence rate or direction is resolvable during the interval between anomalies 30/31 and 21. Thus, apart from a possible correlation in time with a decrease in convergence rate, there is still no simple correlation with detailed structural patterns of compression far inland.

The patterns of magmatism between 80 Ma and 40 Ma are complex. In the western United States, arc-related volcanism waned after about 80 Ma [e.g., Armstrong, 1974; Cross and Pilger, 1978], but intense magmatism occurred in Colorado from 70 to 55 Ma, followed by an absence of volcanism until 40 Ma. From Idaho northward, igneous activity continued from 60 to 41 Ma with little interruption; from southern Arizona southward, it continued from 67 Ma until Miocene time, but its distribution varied. The spatial and geochemical patterns of volcanism during Late Cretaceous and Paleogene time, including the absence of magmatism from about 75 to 55 Ma ("Laramide igneous gap" [e.g., Coney and Reynolds, 1977]) have been inferred to reflect a progressive shallowing of the dip of the subducted slab and resultant "sweep" of the arc eastward in the region south and west of the Colorado Plateau [e.g., Burchfiel and Davis, 1975; Coney and Reynolds, 1977; Cross and Pilger, 1978; Keith, 1978, 1982; Lipman, 1980; Lipman et al., 1971]. The physical distribution of volcanism, if linked to possible segmentation of the subducted Farallon plate, would then be due to the same variety of causes contributing to the segmentation of subducting plates, as discussed above. Hence the times at which the dip of individual slab segments might have changed would be related to changes

in these other factors but not necessarily to changes in Farallon-North America convergence velocity. The time at which the slab is interpreted to have begun to steepen again is pre-55 Ma in Wyoming and Idaho, younging to post-40 Ma toward the south [Lipman, 1980]. This diachroneity and southward progression of volcanism is difficult to associate with the motion of any features whose position can be resolved on the subducted Farallon plate.

The post-40 Ma magmatic patterns in the southwestern United States have been interpreted to suggest several different trends not always related to relative plate motions. Among the proposed trends are a westward migration of arc-related magmatism, inferred to result from a steepening of the subducted slab [Coney and Reynolds, 1977; Keith, 1978], southward and westward convergence of magmatism upon the Lake Mead region of southern Nevada [Anderson, 1981], and northward migration of volcanism inferred to have been triggered by the passage of the escarpment of the subducted Mendocino fracture zone beneath North America [Glazner and Supplee, 1982]. Our ability to evaluate the correlations between these later volcanic patterns and the plate motions is hindered mainly by the variety of scenarios permitted by the igneous data.

CONCLUSIONS

The uncertainties in the relative positions of the Kula, Pacific, and Farallon/Vancouver plates with respect to North America can be divided into two categories: (1) numerical uncertainties derived from small misfits of marine magnetic anomalies and fracture zones, for times at which the basic plate configurations are believed to be understood, and (2) uncertainties in the basic plate configurations themselves, which arise from lack of data and cannot be expressed numerically. In this paper we use a global plate reconstruction circuit, and its uncertainties, to quantify the uncertainties in some problems of the first category, including the history of total Pacific-North America plate boundary motion in late Tertiary time and rates and directions of Farallon-North America, Vancouver-North America, and Pacific-North America motion in early Tertiary time. We find qualitative agreement with the results of previous workers who used fixed hotspot reconstructions to study these problems, but we also find that small changes in velocity and/or position often cannot be resolved, within the uncertainties, to the degree with which they have been used in previous geologic interpretation. Resolution of the reconstructions varies with time but lies generally within the following limits: late Tertiary positions, ±140 km; late Tertiary average velocities, 25%; early Tertiary positions, ±600 km; early Tertiary average velocities, 60%.

The early Tertiary position of the Kula-Farallon ridge relative to North America, the age of Farallon or Kula plate crust subducted under North America during the Laramide orogeny, and the position of major features on this Farallon or Kula plate crust cannot be constrained tightly using plate reconstructions. In particular, the lack of detailed knowledge of the Late Cretaceous configurations of the Farallon and Kula plates permits a variety of different possibilities for which the uncertainties cannot be quantified.

For the interval between anomalies 21 and 18 (49 to 42 Ma), however, significant changes in rate, with possible consequences for the tectonics of western North America, can be resolved. Pacific-North America and Farallon (Vancouver)-North America velocities were slower than have been generally reported. The decrease in Farallon-North America and Pacific-North America relative velocities occurred toward the beginning of this interval, prior to the 43 Ma age of the Hawaiian-Emperor bend, and earlier than recognized in previous studies of Farallon-North America motion.

The unacceptable overlap of Pacific Ocean floor on continental rock of northern Baja California, first noted by Atwater [1970] and found in subsequent studies [e.g., Atwater and Molnar, 1973; Engebretson et al., 1985] is calculated to be at least 340±200 km at anomaly 10 time (30 Ma). Crustal extension in northern Mexico, analogous to that in the Basin and Range province, might explain this discrepancy.

Acknowledgments. We thank T. Atwater for continued interest in this work and for providing a preprint of her DNAG paper well in advance of publication. Jeff Severinghaus provided magnetic anomaly identifications in advance of publication and a preprint of work in progress. We thank T. Atwater (especially), R. Carlson, M. Debiche, and J. Dewey for reviewing the

manuscript. This research was supported in part by NSF grant OCE-8400090. J. M. Stock's graduate studies at M.I.T. were supported by a Fannie and John Hertz Foundation Fellowship.

REFERENCES

Anderson, R. E., Structural ties between the Great Basin and Sonoran Desert sections of the Basin and Range Province, Tectonic Framework of the Mojave and Sonoran Deserts, California and Arizona, edited by K. A. Howard, M. D. Carr, and D. M. Miller, U.S. Geol. Surv. Open File Rep., 81-503, 4-6, 1981.

Armstrong, R. L., Sevier orogenic belt in Nevada and Utah, Geol. Soc. Am. Bull., 79, 429-458, 1968.

Armstrong, R. L., Magmatism, orogenic timing, and orogenic diachronism in the Cordillera from Mexico to Canada, Nature, 247, 348-351, 1974.

Atwater, T., Implications of plate tectonics for the Cenozoic tectonic evolution of western North America, Geol. Soc. Am. Bull., 81, 3513-3536, 1970.

Atwater, T., Plate tectonic history of the northeast Pacific and western North America, in The Eastern Pacific Ocean and Hawaii, Geology of North America, vol. N, edited by D. M. Hussong, E. L. Winterer, and R. W. Decker, Geological Society of America, Boulder, Colo., in press, 1988.

Atwater, T., and H. W. Menard, Magnetic lineations in the northeast Pacific, Earth Planet. Sci. Lett., 7, 445-450, 1970.

Atwater, T., and P. Molnar, Relative motion of the Pacific and North American plates deduced from sea-floor spreading in the Atlantic, Indian, and South Pacific oceans, Proceedings of the Conference on Tectonic Problems of the San Andreas Fault System, edited by R. Kovach and A. Nur, Stanford Univ. Publ. Geol. Sci., 16, 136-148, 1973.

Atwater, T., and J. Severinghaus, Propagating rifts, overlapping spreading centers, and duelling propagators in the northeast Pacific magnetic anomaly record, Eos Trans. AGU., 68, 1493, 1987.

Atwater, T., and J. P. Severinghaus, Tectonic map of the North Pacific, in The Eastern Pacific Ocean and Hawaii, Geology of North America, vol. N, edited by E. L. Winterer, D. M. Hussong, and R. W. Decker, Geological Society of America, Boulder, Colo., in press, 1988.

Beck, M. E., Jr., Introduction to the special issue on correlations between plate motions and Cordilleran tectonics, Tectonics, 3, 103-105, 1984.

Berggren, W. A., D. V. Kent, J. J. Flynn, and J. A. van Couvering, Cenozoic geochronology, Geol. Soc. Am. Bull., 96, 1407-1418, 1985.

Bullard, E. E., J. E. Everett, and A. G. Smith, The fit of the continents around the Atlantic, Philos. Trans. R. Soc. London, Ser. A., 258, 41-51, 1965.

Burchfiel, B. C., and G. A. Davis, Nature and controls of Cordilleran orogenesis, western United States: Extensions of an earlier synthesis, Am. J. Sci., 275-A, 363-396, 1975.

Burke, K., W. S. F. Kidd, and J. T. Wilson, Relative and latitudinal motion of Atlantic hotspots, Nature, 245, 133-137, 1973.

Byrne, T., Late Paleocene demise of the Kula-Pacific spreading center, Geology, 7, 341-344, 1979.

Cande, S. C., and J. C. Mutter, A revised interpretation of the oldest sea floor spreading anomalies between Australia and Antarctica, Earth Planet. Sci. Lett., 58, 151-160, 1982.

Caress, D. W., H. W. Menard, and R. N. Hey, Eocene reorganization of the Pacific-Farallon spreading center north of the Mendocino fracture zone, J. Geophys. Res., 93, 2813-2838, 1988.

Carlson, R. L., Cenozoic convergence along the California coast: A qualitative test of the hot-spot approximation, Geology, 10, 191-196, 1982.

Chang, T., On the statistical properties of estimated rotations, J. Geophys. Res., 92, 6319-6330, 1987.

Chapin, C. E., and S. M. Cather, Eocene tectonics and sedimentation in the Colorado Plateau-Rocky Mountain area, in Rocky Mountain Foreland Basins and Uplifts, edited by J. D. Lowell, pp. 33-56, Rocky Mountain Association of Geologists, Denver, Colo., 1983.

Chase, C. G., Plate kinematics: The Americas, East Africa, and the rest of the world, Earth Planet. Sci. Lett., 37, 355-368, 1978.

Clague, D. A., and G. B. Dalrymple, The Hawaiian-Emperor volcanic chain, I, Geologic evolution, in Geology of North America, Geological Society of America, Boulder, Colo., in press, 1988.

Clark, J. C., E. E. Brabb, H. G. Greene, and D. C. Ross, Geology of Point Reyes peninsula and implications for San Gregorio fault history, in Tectonics and Sedimentation Along the California Margin, Publ. 38, edited by J. K. Crouch and S. B. Bachman, pp. 67-86, Pacific Section, Society of Economic Paleontologists and Mineralogists, Bakersfield, Calif., 1984.

Coney, P. J., Cordilleran tectonics and North American plate motion, Am. J. Sci., 272, 603-628, 1972.

Coney, P. J., Mesozoic-Cenozoic Cordilleran plate tectonics,Cenozoic Tectonics and Regional Geophysics of the Western Cordillera, edited by R. B. Smith and G. P. Eaton, Mem. Geol. Soc. Am., 152, 33-50, 1978.

Coney, P. J., and S. J. Reynolds, Cordilleran Benioff zones, Nature, 270, 403-406, 1977.

Cross, T. A., and R. H. Pilger, Jr., Constraints on absolute motion and plate interaction inferred from Cenozoic igneous activity in the western United States, Am. J. Sci., 278, 865-902, 1978.

Dalziel, I. W. D., West Antarctica: Problem child of Gondwanaland, Tectonics, 1, 3-19, 1982.

DeMets, C., R. G. Gordon, S. Stein, and D. F. Argus, A revised estimate of Pacific-North America motion and implications for western North America plate boundary zone tectonics, Geophys. Res. Lett., 14(9), 911-914, 1987.

Dickinson, W., Cenozoic plate tectonic setting of the Cordilleran region in the United States, in Cenozoic Paleogeography of the Western United States, Pacific Coast Paleogeography Symposium 3, edited by J. M. Armentrout, M. R. Cole, and H. TerBest, Jr., pp. 1-13, Pacific Section, Society of Economic Paleontologists and Mineralogists, Bakersfield, Calif., 1979.

Dickinson, W., and W. S. Snyder, Plate tectonics of the Laramide Orogeny, Laramide Folding Associated with Basement Block Faulting in the Western United States, edited by V. Matthews, III, Mem. Geol. Soc. Am., 151, 355-366, 1978.

Dickinson, W., and W. S. Snyder, Geometry of triple junctions related to the San Andreas transform, J. Geophys.

Res., 84, 561-572, 1979.
Dickinson, W., M. A. Klute, M. J. Hayes, S. U. Janecke, E. R. Lundin, M. A. McKittrick, and M. D. Olivares, Paleogeographic and paleotectonic setting of Laramide sedimentary basins in the central Rocky Mountain region, Geol. Soc. Am. Bull., 100, 1023-1039, 1988.
Duncan, R. A., Hotspots in the southern oceans-- An absolute frame of reference for motion of the Gondwana continents, Tectonophysics, 74, 29-42, 1981.
Engebretson, D. C., A. Cox, and R. G. Gordon, Relative motions between oceanic plates of the Pacific Basin, J. Geophys. Res., 89, 10,291-10,310, 1984a.
Engebretson, D. C., A. Cox, and G. A. Thompson, Correlation of plate motions with continental tectonics: Laramide to Basin-Range, Tectonics, 3, 115-120, 1984b.
Engebretson, D. C., A. Cox, and R. G. Gordon, Relative motions between oceanic and continental plates in the Pacific Basin, Spec. Pap. Geol. Soc. Am., 206, 1985.
England, P., and R. Wortel, Some consequences of the subduction of young slabs, Earth Planet. Sci. Lett., 47, 403-415, 1980.
Fitzgerald, P. G., M. Sandiford, P. J. Barrett, and A. J. W. Gleadow, Asymmetric extension associated with uplift and subsidence in the Transantarctic Mountains and Ross Embayment, Earth Planet. Sci. Lett., 81, 67-78, 1987.
Fox, K. F., Jr., Melanges and their bearing on late Mesozoic and Tertiary subduction and interplate translation at the western edge of the North American plate, U. S. Geol. Surv. Prof. Pap., 1198, 1983.
Glazner, A. F., and J. A. Supplee, Migration of Tertiary volcanism in the southwestern United States and subduction of the Mendocino Fracture Zone, Earth Planet. Sci. Lett., 60, 429-436, 1982.
Graham, S. A., and W. R. Dickinson, Evidence for 115 kilometers of right slip on the San Gregorio-Hosgri fault trend, Science, 199, 179-181, 1978.
Gries, R., North-south compression of Rocky Mountain foreland structures, in Rocky Mountain Foreland Basins and Uplifts, edited by J. D. Lowell, pp. 9-32, Rocky Mountain Association of Geologists, Denver, Colo., 1983.
Hamilton, W., Tectonics of Antarctica, Tectonophysics, 4, 555-568, 1967.
Hamilton, W., Mesozoic tectonics of the western United States, in Mesozoic Paleogeography of the Western United States, Pacific Coast Paleogeography Symposium 2, edited by D. G. Howell and K. A. McDougall, pp. 33-70, Pacific Section, Society of Economic Paleontologists and Mineralogists, Bakersfield, Calif., 1978.
Harland, W. B., A. V. Cox, P. G. Llewellyn, A. G. Picton, A. G. Smith, and A. Walters, A Geologic Time Scale, Cambridge University Press, New York, 1982.
Hayes, D. E., and W. C. Pitman III, Magnetic lineations in the North Pacific, Geological Investigations of the North Pacific, edited by J. D. Hays, Mem. Geol. Soc. Am., 126, 291-314, 1970.
Hellinger, S. J., The uncertainties of finite rotations in plate tectonics, J. Geophys. Res., 86, 9312-9318, 1981.
Henderson, L. J., R. G. Gordon, and D. C. Engebretson, Mesozoic aseismic ridges on the Farallon plate and southward migration of shallow subduction during the Laramide orogeny, Tectonics, 3, 121-132, 1984.
Hilde, T. W. C., N. Isezaki, and J. M. Wageman, Mesozoic sea-floor spreading in the North Pacific, in The Geophysics of the Pacific Ocean Basin and Its Margins, Geophys. Monogr. Ser., vol. 19, edited by G. H. Sutton, M. H. Manghnani, and R. Moberly, pp. 205-226, AGU, Washington, D. C., 1976.
Jordan, T. E., B. L. Isacks, R. W. Allmendinger, J. A. Brewer, V. A. Ramos, and C. J. Ando, Andean tectonics related to geometry of subducted Nazca plate, Geol. Soc. Am. Bull., 94, 341-361, 1983.
Jurdy, D. M., The subduction of the Farallon plate beneath North America as derived from relative plate motions, Tectonics, 3, 107-113, 1984.
Jurdy, D. M., and M. Stefanick, Errors in plate rotations as described by covariance matrices and their combination in reconstructions, J. Geophys. Res., 92, 6310-6318, 1987.
Kamp, P. J. J., and P. G. Fitzgerald, Geologic constraints on the Cenozoic Antarctica-Australia-Pacific relative plate motion circuit, Geology, 15, 694-697, 1987.
Keith, S. B., Paleosubduction geometries inferred from Cretaceous and Tertiary magmatic patterns in southwestern North America, Geology, 6, 516-521, 1978.
Keith, S. B., Paleosubduction rates determined from K_2O/SiO_2 ratios in magmatic rocks and their application to Cretaceous and Tertiary tectonic patterns in southwestern North America, Geol. Soc. Am. Bull., 93, 524-532, 1982.
Kent, D. V., and F. M. Gradstein, A Cretaceous and Jurassic geochronology, Geol. Soc. Am. Bull., 96, 1419-1427, 1985.
Klitgord, K., and H. Schouten, Plate kinematics of the central Atlantic, in The Geology of North America, vol. M, The Western North Atlantic Region, edited by P. R. Vogt and B. E. Tucholke, pp. 351-378, Geological Society of America, Boulder, Colo., 1986.
König, M., Geophysical investigations of the northern continental margin of Antarctica, PhD dissertation, Columbia University, New York, 1980.
Lipman, P. W., Cenozoic volcanism in the western United States: Implications for continental tectonics, in Continental Tectonics, pp. 161-174, National Research Council Geophysics Study Committee, Washington, D. C., 1980.
Lipman, P. W., H. J. Prostka, and R. L. Christiansen, Evolving subduction zones in the western United States, as interpreted from igneous rocks, Science, 174, 821-825, 1971.
Livaccari, R. F., K. Burke, and A. M. C. Sengor, Was the Laramide orogeny related to the subduction of an oceanic plateau?, Nature, 289, 276-278, 1981.
Lonsdale, P., Paleogene history of the Kula plate: Offshore evidence and onshore implications, Geol. Soc. Am. Bull., 100, 733-754, 1988.
Luyendyk, B. P., M. J. Kamerling, R. R. Terres, and J. S. Hornafius, Simple shear of southern California during Neogene time suggested by paleomagnetic vectors, J. Geophys. Res., 90, 12,454-12,466, 1985.
Mammerickx, J., and G. Sharman, Tectonic evolution of the North Pacific during the Cretaceous Quiet Period, J. Geophys. Res., 93, 3009-3024, 1988.
Matthews, V., III, Pinnacles-Neenach correlation: A restriction for models of the origin of the Transverse Ranges and the Big Bend in the San Andreas fault, Geol. Soc. Am. Bull., 84, 683-688, 1973.
Matthews, V., III, Correlation of Pinnacles and Neenach volcanic formations and their bearing on the San Andreas

fault system, Am. Assoc. Pet. Geol. Bull., 60, 2128-2141, 1976.
McKenzie, D. P., and J. G. Sclater, The evolution of the Indian Ocean since the Late Cretaceous, Geophys. J. R. Astron. Soc., 25, 437-528, 1971.
McKenzie, D. P., D. Davies, and P. Molnar, Plate tectonics of the Red Sea and East Africa, Nature, 226, 243-248, 1970.
Menard, H. W., Fragmentation of the Farallon plate by pivoting subduction, J. Geol., 86, 99-110, 1978.
Minster, J. B., and T. H. Jordan, Present-day plate motions, J. Geophys. Res., 83, 5331-5351, 1978.
Molnar, P., and T. Atwater, The relative motion of hot-spots in the mantle, Nature, 246, 288-291, 1973.
Molnar, P., and T. Atwater, Interarc spreading and Cordilleran tectonics as alternates related to the age of subducted oceanic lithosphere, Earth Planet. Sci. Lett., 41, 330-340, 1978.
Molnar, P., and J. Francheteau, The relative motion of "hot spots" in the Atlantic and Indian Oceans during the Cenozoic, Geophys. J. R. Astron. Soc., 43, 763-774, 1975.
Molnar, P., and H. Lyon-Caen, Some simple physical aspects of the support, structure, and evolution of mountain belts, Spec. Pap. Geol. Soc. Am., 218, 179-207, 1988.
Molnar, P., and J. M. Stock, A method for bounding uncertainties in combined plate reconstructions, J. Geophys. Res., 90, 12,537-12,544, 1985.
Molnar, P., and J. M. Stock, Relative motions of hotspots in the Pacific, Atlantic, and Indian Oceans since Late Cretaceous time, Nature, 327, 587-591, 1987.
Molnar, P., T. Atwater, J. Mammerickx, and S. M. Smith, Magnetic anomalies, bathymetry, and the tectonic evolution of the South Pacific since the late Cretaceous, Geophys. J. R. Astron. Soc., 40, 383-420, 1975.
Molnar, P., F. Pardo-Casas, and J. M. Stock, Uncertainties in the reconstructions of the Indian, African, and Antarctic plates since Late Cretaceous time, Basin Res., 1, 23-40, 1988.
Morgan, W. J., Convection plumes in the lower mantle, Nature, 230, 42-43, 1971.
Morgan, W. J., Hotspot tracks and the opening of the Atlantic and Indian Oceans, in The Sea, vol. 7, The Oceanic Lithosphere, edited by C. Emiliani, pp. 443-447, Wiley Interscience, New York, 1981.
Morgan, W. J., Hotspot tracks and the early rifting of the Atlantic, Tectonophysics, 94, 123-139, 1983.
Nelson, M., R. McCaffrey, and P. Molnar, Source parameters for 11 earthquakes in the Tien Shan, central Asia, determined by P and S waveform inversion, J. Geophys. Res., 92, 12,629-12,648, 1987.
Nishimura, C., D. S. Wilson, and R. N. Hey, Pole of rotation analysis of present-day Juan de Fuca plate motion, J. Geophys. Res., 89, 10,283-10,290, 1984.
Pardo-Casas, F., and P. Molnar, Relative motion of the Nazca (Farallon) and South American plates since Late Cretaceous time, Tectonics, 6, 233-248, 1987.
Pilger, R. H., A method for finite plate reconstructions, with applications to Pacific-Nazca plate evolution, Geophys. Res. Lett., 5, 469-472, 1978.
Pilger, R. H., Plate reconstructions, aseismic ridges, and low-angle subduction beneath the Andes, Geol. Soc. Am. Bull., 92, 448-456, 1981.
Pilger, R. H., Cenozoic plate kinematics, subduction and magmatism: South American Andes, J. Geol. Soc. London, 141, 793-802, 1984.
Pitman, W. C., E. M. Herron, and J. R. Heirtzler, Magnetic anomalies in the Pacific and seafloor spreading, J. Geophys. Res., 73, 2069-2085, 1968.
Pollitz, F., Episodic North America and Pacific plate motions, Tectonics, 7, 711-726, 1988.
Rea, D. K., and J. M. Dixon, Late Cretaceous and Paleogene tectonic evolution of the North Pacific Ocean, Earth Planet. Sci. Lett., 65, 145-166, 1983.
Rea, D. K., and R. A. Duncan, North Pacific plate convergence--A quantitative record of the past 140 m.y., Geology, 14, 373-376, 1986.
Rosa, J. W. C., and P. Molnar, Uncertainties in reconstructions of the Pacific, Farallon, Vancouver, and Kula plates and constraints on the rigidity of the Pacific and Farallon (and Vancouver) plates between 72 and 35 Ma, J. Geophys. Res., 93, 2997-3008, 1988.
Severinghaus, J., and T. Atwater, Age of lithosphere subducted beneath western North America: Implications for the Neogene seismic history of the Cascadia slab, Eos Trans. AGU, 68, 1467, 1987.
Stein, S., and E. A. Okal, Seismicity and tectonics of the Ninety-East ridge area: Evidence for internal deformation of the Indian plate, J. Geophys. Res., 83, 2233-2245, 1978.
Stock, J. M., and K. V. Hodges, Pre-Pliocene extension around the Gulf of California and the transfer of Baja California to the Pacific plate, in press, Tectonics, 1988.
Stock, J. M., and P. Molnar, Uncertainties in the relative positions of the Australia, Antarctica, Lord Howe, and Pacific plates since the Late Cretaceous, J. Geophys. Res., 87, 4697-4714, 1982.
Stock, J. M., and P. Molnar, Some geometrical aspects of uncertainties in combined plate reconstructions, Geology, 11, 697-701, 1983.
Stock, J. M., and P. Molnar, A revised history of early Tertiary plate motion in the south-west Pacific, Nature, 325, 495-499, 1987.
Tweto, O., Laramide (Late Cretaceous-early Tertiary) orogeny in the Southern Rocky Mountains, Cenozoic History of the Southern Rocky Mountains, edited by B. F. Curtis, Mem. Geol. Soc. Am., 144, 1-44, 1975.
Verplanck, E. P., and R. A. Duncan, Temporal variations in plate convergence and eruption rates in the western Cascades, Oregon, Tectonics, 6, 197-209, 1987.
Wernicke, B. P., G. J. Axen, and J. K. Snow, Basin and range extensional tectonics at the latitude of Las Vegas, Nevada, Geol. Soc. Am. Bull., 100, 1738-1757, 1988.
Wiens, D. A., et al., A diffuse plate boundary model for Indian Ocean tectonics, Geophys. Res. Lett., 12, 429-432, 1985.
Wilson, J. T., A possible origin of the Hawaiian Islands, Can. J. Phys., 41, 863-870, 1963.
Woods, M. T., and G. F. Davies, Late Cretaceous genesis of the Kula plate, Earth Planet. Sci. Lett., 58, 161-168, 1982.

P. Molnar and J. M. Stock, Department of Earth, Atmospheric, and Planetary Sciences, Massachusetts Institute of Technology, Cambridge MA 01239

(Received March 7, 1988;
revised August 10, 1988;
accepted August 12, 1988.)